Challenge Journal of
CONCRETE RESEARCH LETTERS

Vol.13 No.3 (2022)

acoustic emission aerated concrete compressive strength concrete corrosion cracking curing ductility durability energy absorption ferrocement fly ash fracture mechanical properties mortar nanoparticle palm oil fuel ash reinforced concrete self-compacting concrete silica fume strengthening superplasticizer tensile strength workability waste disposal water absorption

ISSN 2548-0928

TULPAR ACADEMIC PUBLISHING

Challenge Journal of Concrete Research Letters

E-mail: *cjcrl@challengejournal.com*

Web page: *cjcrl.challengejournal.com*

TULPAR Academic Publishing
www.tulparpublishing.com

Challenge Journal of Concrete Research Letters

CONTENTS

Research Articles

TULPAR ACADEMIC PUBLISHING

Challenge Journal of Concrete Research Letters

Research Article

Assessing effects of waste coal bottom ash on construction cost of reinforced concrete structures considering experimental data

Memduh Karalar [a,*], Burak Oz [a], Murat Çavuşli [a]

[a] *Department of Civil Engineering, Zonguldak Bülent Ecevit University, İncivez, 67100 Zonguldak, Turkey*

ABSTRACT

In this study, it has been examined whether the bottom ash (BA) released to the nature as waste material from the thermal power plant can be used in reinforced concrete structures (RCS) and how much cost reduction will be caused in construction technology if BA is used in RCS. For this purpose, coal BA produced by Turkey-Zonguldak Cates power plant is mixed in different ratios into the concrete mixture of the beams. The different coal bottom ash ratio (BAR) is used instead of aggregate in the mixture. The beams created for 5 different BARs are subjected to tests and it is observed that the beam with the most critical bending is the beam with 75% coal BA. This BAR is applied to bearing elements of finite element model (FEM) and then current cost of the building and the construction cost used 75% coal BAR are compared with each other. It has been observed that when 75% coal BAR is used instead of aggregate in RCSs, there is a 40% reduction in construction costs. This result is of great importance both for the recycling of BA and for revealing that BA reduces construction costs.

ARTICLE INFO

Article history:
Received 20 April 2022
Revised 20 May 2022
Accepted 14 June 2022

Keywords:
Coal bottom ash
Crack behavior
Construction cost
Construction management
Finite element analysis

1. Introduction

Coal BA is the excellently distributed mineral residue resulting from the incineration of pulverized coal in power plants (PPs) and it is the major quantity of manufacturing leftover in the world. PPs every year, billion tons of coal BA are produced, and it is not recycled in the world. Therefore, coal BA produced in PPs all over our planet destroys our nature every year. Ensuring the recycling of this waste material is of great significance. Coal wastes burned in thermal PPs are transported with water and stored in ash dams. Toxic metals contained in coal ash might spread in the surrounding environment in case of waste leaking or explosion of the waste dams. Many studies have shown that living near coal ash disposal sites increases the risks of cancer and other diseases (Sönmez and Işık 2020). Although the chemical and physical belongings of coal ash make it ideal for a diversity of industrial presentations, it is supposed to compete with other inexpensive materials such as sand and gravel, so it is economical only when transportation and processing costs can be kept low. About three quarters of the coal ash produced in the United States is not recycled for commercial use, but instead is stored in specially designed, permitted dump areas (URL1). Twenty-four percent of the coal ashes obtained from thermal PPs in England is used as BA in lightweight concrete blocks (Aruntaş 2006; Güler et al. 2005; Huang et al. 2019; Hwang and Cortés 2021; Jang and Xing 2020). Additionally, Kaplan and Gültekin (2010) indicated many benefits of using coal waste in recycling in their research (Sönmez and Işık 2020). Many researchers have examined coal BA in the literature so far. Cao et al. (2008) examined utilization of BA from coal-fired PPs in China. It was indicated that the operation of PPs in China should improve to actual state-of-the- art. Careful input control, efficient burn out, and an additional feed of suitable components to improve a high quality of BA with low Loss on Ignition (LOI) will ensure higher standards in the utilization of Chinese BA. For the time being, the best chance is to replace solid clay bricks which become banned from 2007. Yost et al. (2013) examined structural performance of alkali acti-

* *Corresponding author*. Tel.: +90-372-291-2582 ; Fax: +90-372-257-4023 ; E-mail address: memduhkaralar@beun.edu.tr (M. Karalar)
ISSN: 2548-0928 / DOI: https://doi.org/10.20528/cjcrl.2022.03.001

vated BA concrete. The procedures used in this investigation to create alkali activated BA concrete beams were effective in regards to material workability, strength, and stiffness, and conclusively show that BA can be practiced as a viable 100 % substitute for portland cement in the manufacturing of RC structural members. Wang et al. (2016) examined new technology and application of brick making with coal BA. The examination consequences offered that the different technology of brick creation could consume a large amount of BA. Varied amount of cement was simply 8–13%, and the cement rating was 425 #, the amount of BA additives in the composition was also minor, only 0.03–0.05%, for that reason, the charge of the project's creation was clearly lesser, and it exhibited decent financial profit for submission. Karalar (2020) performed experimental and numerical examination on flexural and crack failure of RC beams with BA and BA. In this study, load–deflection graphic for experimental test consequences is very parallel to load–deflection graphic of 3D numerical analyses. Additionally, actual near crack forms are found for experimental and numerical investigations. This obviously shows that FEM may be an exceptional alternative for damaging laboratory tests with conventional variations in the results. Ramachandran et al. investigated strong point and permanence behaviour of BA concrete in sea water surroundings related with normal and superplasticizer concrete. The pH, compressive strength, Half Cell Potential (HCP), Rapid Chloride Permeability Test (RCPT) and carbonation test showed better results in concrete with BA and superplasticizer (FA) (Ramachandran et al. 2017). Dinelli et al. (1996) performed experimental investigation on the use of BA for lightweight precast structural elements. The technical feasibility of the wide use of BA in fundamental concrete in the way of lightweight aggregates and as fine pozzolanic components has been presented by the tests available in this research. Wu et al. (2014) assessed characteristics of CFBC BA and properties of cement-based composites with CFBC BA and coal-fired BA. It was shown that CFBC BA has the potential as an alternative of cementing materials and as an alternative of pozzolan. The primary situation period rises with a growing amount of cement replacement by CFBC BA and coal-fire BA. The lower compressive strength has been gained in mortar with numerous mixtures of coal-fired BA and CFBC BA than the comparable ordinary Portland cement (OPC) mortar. Coal-fired BA can be successfully used in decreasing the length alteration. Nevertheless, CFBC BA would results in a higher length change when adding over 30%. Therefore, the quantity of CFBC BA replacement cement was suggested to be limited below 20%. Besides, there are many studies about coal BA in the literature such as Albitar et al. (2015), Baspinar (2014), Cavusoglu et al. (2021), Dry et al. (2004), Esquinas et al. (2018), Li et al. (2018), Nakamura et al. (2021), Sun et al. (2019), Tan et al. (2019), and Verma et al. (2019).

As realized from these studies, very few investigators were observed the effects of various coal BA ratios on construction cost of RC library buildings in the past. Besides, there are very few studies about the effects of various coal BA ratios on 3D seismic behaviour of library structural elements (beams, columns) in the literature. Therefore, in this study, it is intended to reveal the effects of coal BA contribution on the seismic behavior and construction cost of library structures.

2. Aim of the Study

In this study, to investigate the effects of various coal BA ratios on construction cost of RC buildings is investigated in detail. For this purpose, total 5 various RCBs are created in the research laboratory. Firstly, pure concrete is produced in laboratory. At that point BA is used instead of aggregate in pure concrete and BA added RC is obtained. The BARs used in pure concrete are 25%, 50%, 75% and 100%. Then, these beams are subjected to bending test. The most critical beam (concrete with 75% coal BA) is taken as reference and the properties of this reference concrete material is used for structural elements of a library building to investigate the effects of coal BARs on construction cost of RC buildings. For this purpose, the existing structure has been modeled with the mechanical belongings of the 75% BA substitution and the carrier system has been reanalyzed, except for the foundation system. Then, earthquake analysis has been performed. It is observed that the structure is not damaged in the earthquake when dimensions of the columns and beams in the structure used coal BA added concrete are reduced. Then, the cost has been compared between concrete with 75% BA substitution and without BA in the current design. From this result, it is concluded that when concrete with 75% coal BA is used in RCSs, there will be a significant reduction in the cost of RC library constructions and this recycling will make an important influence to the country's economy.

3. Preparation of RC Beams

In Zonguldak-Turkey, coal is produced since the 1900s and this produced coal is sent to both other provinces and countries. For this reason, a coal-fired thermal power plant (Çates) was established in Zonguldak to turn coal into energy. The waste coal BA produced in this coal-fired thermal power plant is released to nature every day and causes great damage to nature. Therefore, recycling of this coal BA is of great importance both for Turkey's economy and health of people living in located in the Zonguldak. In this study, the contribution of the addition of coal BA, which is waste in nature, to the construction cost of RCSs is investigated both experimentally and numerically. Experimentally, the concrete material is prepared in the laboratory and 0%, 25%, 50%, 75% and 100% coal BA is added instead of aggregate in the prepared concrete materials. As a result of this experiment, the most critical BAR is determined. Details of the concrete samples organized in the research test site are offered in Table 1. As can be realized from Table 1, sample 1 represents pure concrete and other samples represent additive concretes. Coal BA has been used in the concrete mix to replace aggregates of 0-5 mm grain size. Details of the materials used in 5 different concrete beams are presented in Table 2.

Table 1. Concrete samples for various BARs (Karalar 2020).

Sample Number	Statement
1	Pure concrete
2	25% BA
3	50% BA
4	75% BA
5	100% BA

Table 2. Components in the concrete examples and weight per unit of components (Karalar 2020).

Material	Pure	25% BA	50% BA	75% BA	100% BA
Cement (kg)	9.00	9.00	9.00	9.00	9.00
Water (kg)	4.77	4.77	4.77	4.77	4.77
BA (kg)	0.00	3.77	7.54	11.31	15.08
0-5 mm aggregate (kg)	23.14	17.35	11.57	5.78	0.00
5-15 mm aggregate (kg)	12.73	12.73	12.73	12.73	12.73
15-25 mm aggregate (kg)	21.99	21.99	21.99	21.99	21.99
Admixture material (kg)	0.12	0.12	0.12	0.12	0.12
Unit weight of concrete (kg)	71.75	69.74	67.72	65.71	63.69

When Table 2 is observed in detail, it is realized that there is no BA in pure concrete and the BA rates are gradually increased for other concrete samples. According to Table 2, the maximum BAR used in concrete materials instead of aggregate is 100% (15.0832 kg). Total 9 kg cement and 4.77 kg water is used in 5 different concrete materials. In addition, Limak CEM IV / B (P) 32.5 N / R pozzolanic cement is used for 5 different concrete materials. City water is used for the water in the concrete materials. Weber 10 water impermeable admixture is used as an additive to increase the consistency of the concrete. For the RC samples, BA is obtained from Zonguldak coal-fired thermal power plant and added to the concrete materials. The capacity of this coal-fired thermal power plant is 2x150 MW. About 1.500.000 tons of coal is burned annually in this factory. Conclusions, tons of ash are formed annually. 5 different concrete sample mixes are mixed in the concrete mixer and the concrete consistency is adjusted (Fig. 1).

After the concrete samples are prepared, they are subjected to slump test (Fig. 2). The slump test results of concrete samples with 5 different BARs are given in Fig. 3. While the experimental consequences are observed, it is determined that while BAR in the concrete sample increased, the slump values of the concrete increased. 4.9 cm slump value is obtained for pure concrete and 5.5 cm slump value is observed for 25% BA. This result shows the effect of BA on concrete consistency. In addition, 18.8 cm slump value is acquired for 50% BA and 25 cm slump value is observed for 75% BA. Finally, 4.1 cm slump value is obtained for concrete with 100% BA. It is clearly seen from these results that when the BAR used in concrete is increased from 0% to 75%, the consistency of concrete gradually increased. This result obviously shows the effect of BA on the consistency of the concrete material (Karalar 2020).

Fig. 2 shows that how concrete beams and beam molds are prepared in the laboratory. 5 different RC beam molds are prepared in a private laboratory. The dimensions of the 5 different beam molds are equal and the beam mold dimensions are 300x400x2000 mm. Total 10 different stirrups are used in concrete beams and the distances between stirrups are 200 mm. Besides, the diameter of stirrups is 8 mm. 2 compression reinforcements are placed on the concrete beams to ensure stirrup connections. These compression reinforcement bars have a diameter of 12 mm. In addition, 3 tension reinforcements are placed at the bottom of the beam molds and the diameter of these tension bars is 12 mm. In Figs. 3 and 4, pouring concrete materials into beam molds and performing vibration process are shown in detail. After a total of 5 different beams are prepared in the laboratory, a total of 28 days are waited for the concrete to reach the desired hardness, and after 28 days, the beam molds are removed (Fig. 4) (Karalar 2020).

Fig. 1. Preparation of concrete material in the laboratory.

Fig. 2. Preparation of molds for concrete beams (Karalar 2020).

Fig. 3. Pouring the concrete material into the beam molds and performing the vibration process (Karalar 2020).

Fig. 4. View of prepared concrete beams (Karalar 2020).

4. Experimental Test Set-up and Results

In this division, the test set-up is shown in Fig.5 (Karalar 2020). 5 different RCBs prepared in the special laboratory are placed in the flexure-crack device shown in Fig. 6 and subjected to flexure and crack tests. Flexure and crack test results are offered in Fig. 7. The crack results of the beam prepared with pure concrete are shown in Figs. 7a and 7b. According to Figs. 7a and 7b, the maximum crack width for pure concrete is 3.17 cm. Besides, the maximum crack length for pure concreted beam is 43 cm. In Figs. 7c and 7d, the flexure and crack test results of the beam prepared by adding 25% coal BA into concrete instead of aggregate are presented. According to Figs. 7c and 7d, maximum crack width is 2.68 cm and maximum crack length is 39 cm. From this result, it is seen that when coal BA is added to the concrete, the crack width and crack length decrease. In Figs 7e and 7f, flexure and crack test results of the beam prepared by adding 50% coal BA into concrete instead of aggregate are shown in detail. According to Figs. 7e and 7f, the maximum crack width on the beam is 2.05 cm and the maximum crack length is 32 cm. In Figs. 7g and 7h, test results of the beam prepared by adding 75% coal BA to the aggregate in the concrete are presented. If 75% of coal BA is added instead of aggregate in the concrete inside the beam, the maximum crack width is 1.66 cm and the maximum crack length is 24 cm. Finally, for the beam where 100% coal BA is used instead of the aggregate in the concrete, the maximum crack width is 2.19 cm and the maximum crack length is 31 cm (Figs. 7i and 7j). It is clear from these results that the most critical threshold value for 5 different coal BARs (0%, 25%, 50%, 75%, 100%) used instead of aggregate in concrete is 75% coal BAR. If this ratio is used instead of aggregate in concrete, it causes the smallest crack width and crack length in beam elements. From this result, it is concluded that using 75% coal BAR in RCSs may cause less damage in the RC structures (Karalar 2020).

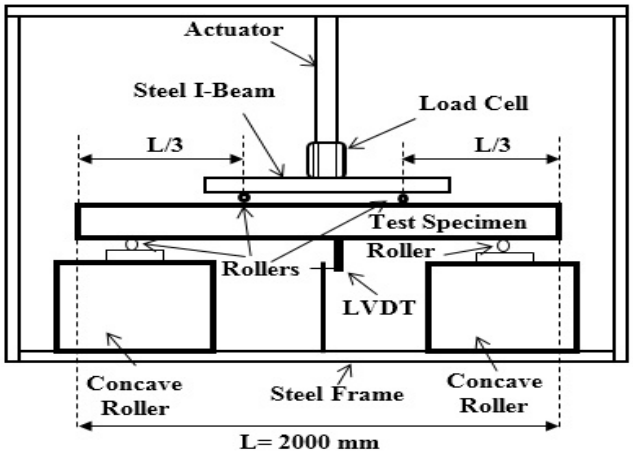

Fig. 5. Loading configuration for static testing (Karalar et al. 2020).

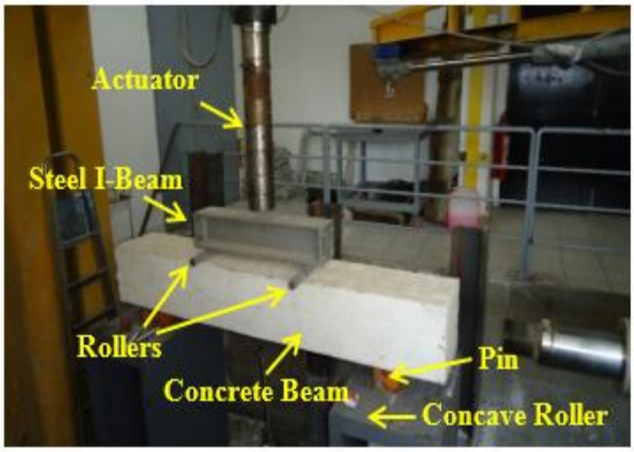

Fig. 6. Static testing apparatus (Karalar et al. 2020).

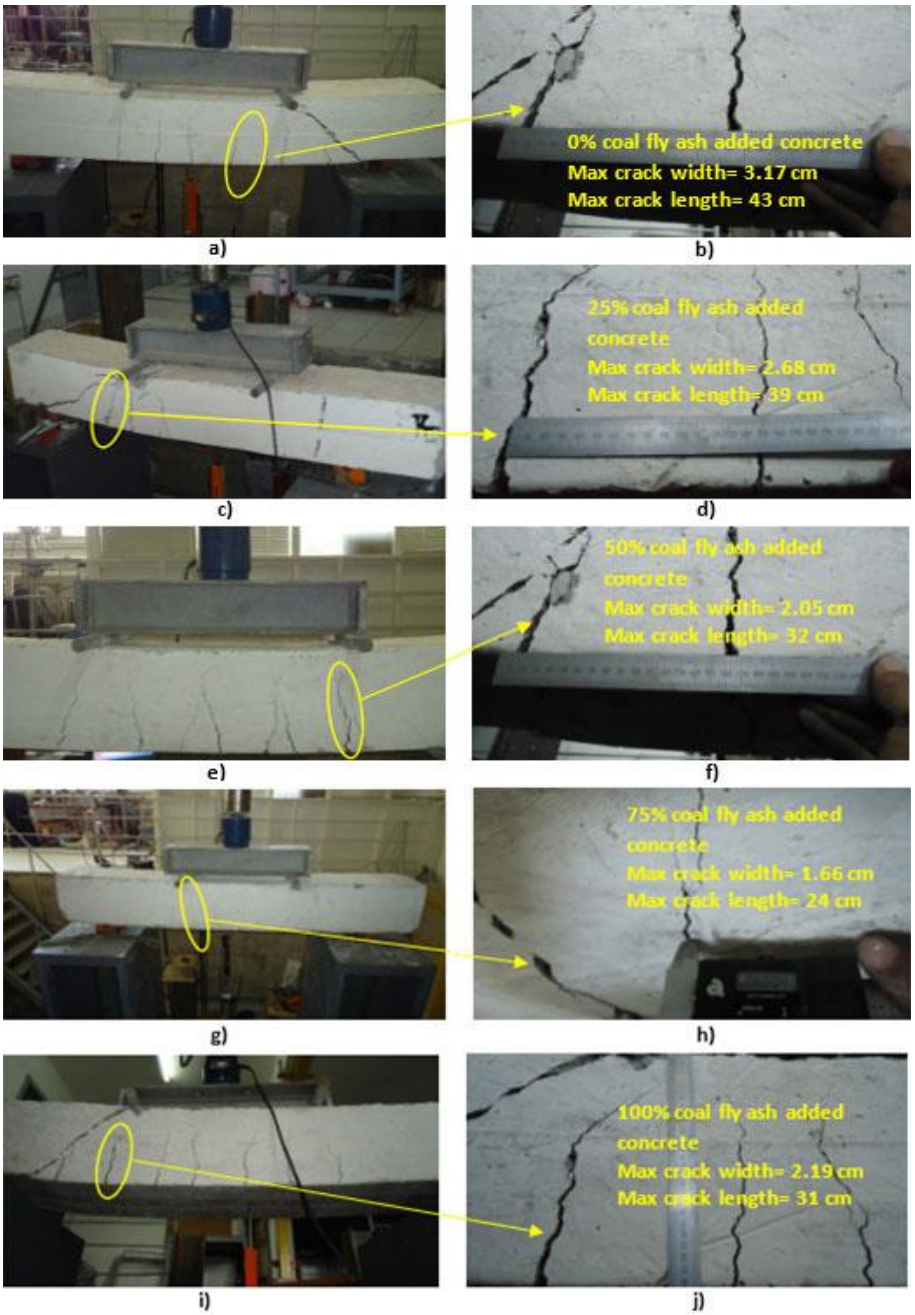

Fig. 7. Crack test results of 5 different beams (Karalar 2020).

5. 3D Modelling RC Building and Earthquake Analysis Results

Library structures are one of the important structures that people use frequently. Hundreds of people enter and exit the library structures every day. Controlling the seismic safety of these structures is of great importance for the safety and health of people. Therefore, library structure is used for numerical analysis in this study. In this part, it is intended to observe whether the building will survive under different ground motions and various coal BARs in the concrete material. For this purpose, firstly, current situation of library building is modelled according to original building project. 4 five multi-story RC building is chosen for 3D modelling and SAP2000 is developed whereas demonstrating of this RC building. Whereas demonstrating this RC building, 6 dissimilar columns are demarcated to the SAP2000 and thickness-elevation of these columns are demarcated as 70x70 cm, 60x60 cm, 50x50 cm, respectively (Fig. 8). Furthermore, there is a spherical column in the building and its diameter is demarcated as 50 cm. Then, width-height of beams used in the SAP2000 is demarcated as 40x70 cm, 35x70 cm, 30x70 cm, 40x60 cm, 40x50 cm, 30x50 cm, respectively (Fig. 8). Class of concrete are demarcated as C35 and this rate is gotten from original structure project. Overall sight of library construction is presented in Fig. 9.

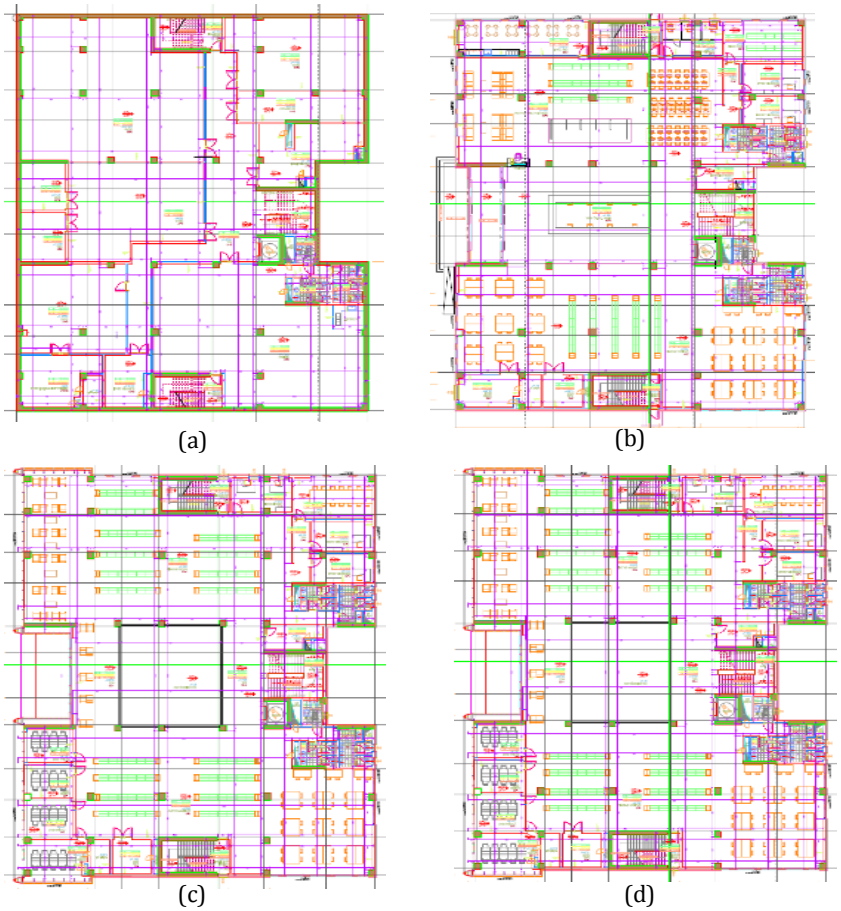

Fig. 8. Divisions of building levels: a) First level; b) Second level; c) Third level; d) Fourth level.

Fig. 9. General view of library building.

In the library RC building, there are entirely 2 dissimilar shear walls and their thicknesses are 20 cm and 25 cm. Moreover, thickness of ground layer is taken as 20 cm for all floors. Altitude of separately ground is taken as 3 m and there are completely 4 floors in the building. Additionally, inflexible diaphragms are formed in the building allowing for restraint z axis. At that point, nonlinear time history analyses are done allowing directing incorporation result type. Thus, Hilber-Hughes-Taylor method is chosen in the analyses and its gamma and beta value is chosen as 0.5 and 0.25, respectively. 3D model of building is presented in Fig. 10. Earthquake accelerations of 10 various earthquakes are used in 3D earthquake analyses. Mechanical properties of various earthquakes are presented in Table 3.

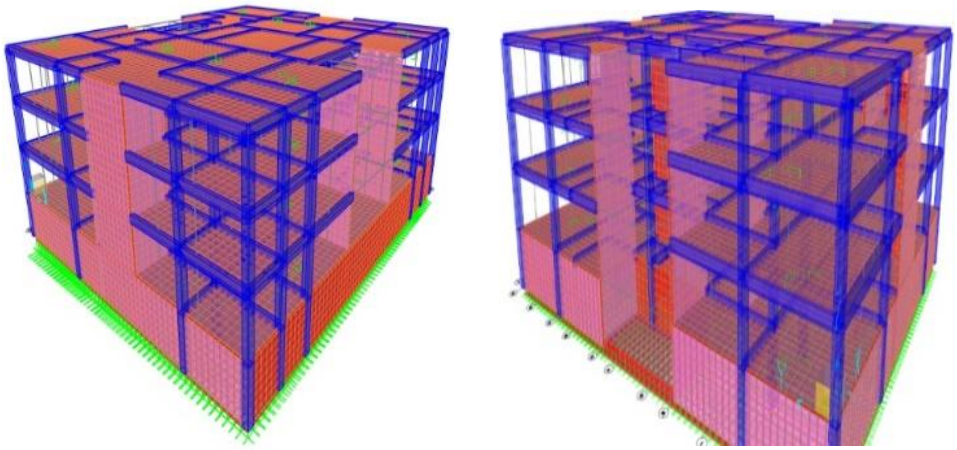

(a) (b)

Fig. 10. 3D model of library building: a) Right view; b) Left view.

Table 3. Mechanical properties of various earthquakes.

Earthquake Record Station	*d* (km)	PGA	PGV	Ap/Vp	TPV	TP
1999 Chi-Chi Earthquake 1	17.8	0.17	59	2.83	6.5	6.0
1999 Chi-Chi Earthquake 2	18.1	0.25	46	5.33	1.4	1.3
1979 Imperial Valley Earthquake 1	0.5	0.30	91	3.23	3.0	3.1
1979 Imperial Valley Earthquake 2	0.6	0.46	109	4.14	3.2	3.8
1979 Imperial Valley Earthquake 3	1.0	0.38	91	4.10	3.4	3.9
1995 Kobe Earthquake	0.6	0.60	74	7.95	0.8	1.4
1989 Loma Prieta Earthquake	5.1	0.48	45	10.46	0.8	0.7
1986 North Palm Spring Earthquake	8.2	0.59	73	7.93	1.1	1.4
1994 Northridge Earthquake 1	7.1	0.45	93	4.75	2.0	3.2
1994 Northridge Earthquake 2	7.1	0.33	67	4.83	1.8	1.9

3D earthquake analysis outcomes are offered in Table 4. While Table 4 is observed, the earthquake analysis consequences for the current situation of RC library structure and the earthquake analysis results for the coal BA added situation of RC structure are presented separately. 3D earthquake analyses are performed under 10 different earthquakes. Damages in the building were evaluated by examining the stresses and displacements that occurred in the beams and columns in the building after the earthquake analyses. According to 10 different earthquake analysis results, no damage is obtained in the structural elements for the current situation of the building. From this result, it is established that the existing bearing columns and beams are sized appropriately for these earthquakes. Besides, provided that the dimensions of the existing bearing elements of the structure remain constant, it has been observed that if 75% of the coal BA is added to the aggregate in the bearing elements of the structure, no damage will occur for 10 different earthquakes. When the size of the columns and beams is reduced by 10% ratio for the structure with coal BA, there is no damage to the building for 10 different earthquakes. No damage is observed in the structure for 10 different earthquakes in the case of reducing the dimensions of the carrier elements by 20%, 30%, 40% ratios for the structure with coal BA. However, if the dimensions of the bearing elements for the coal BA added structure are reduced by 50% ratio, the structure is damaged for 1999 Chi-Chi earthquake, 1989 Loma Prieta earthquake, 1986 North Palm earthquake, 1994 Northridge earthquake. In this case, it is concluded that the reduction ratio that should be taken as reference is 40% ratio. From this result, it is concluded that if 75% ratio of coal BA is used instead of aggregate in the library structures, the carrying ele-

ments of the structure can be reduced by 40% ratio, and if the carrier elements are reduced by 40% ratio, the structure may resist earthquakes. It is understood from this result that if 75% ratio of coal BA waste material is used in concrete material of RC structures, it will cause a significant decrease in the cost of the building.

Table 4. Earthquake analysis results for current situation and coal BA added situation.

Earthquake	Current situation of structure	Reduction ratio for structural elements (beams and columns)					
		10%	20%	30%	40%	50%	60%
1999 Chi-Chi Earthquake 1	+	+	+	+	+	-	-
1999 Chi-Chi Earthquake 2	+	+	+	+	+	-	-
1979 Imperial Valley Earthquake 1	+	+	+	+	+	+	-
1979 Imperial Valley Earthquake 2	+	+	+	+	+	+	-
1979 Imperial Valley Earthquake 3	+	+	+	+	+	+	-
1995 Kobe Earthquake	+	+	+	+	+	+	-
1989 Loma Prieta Earthquake	+	+	+	+	+	-	-
1986 North Palm Spring Earthquake	+	+	+	+	+	-	-
1994 Northridge Earthquake 1	+	+	+	+	+	-	-
1994 Northridge Earthquake 2	+	+	+	+	+	+	-

6. The Effect of Using 75% Coal BA in Concrete on Construction Costs

Depending on the use of coal in the thermal PPs in Turkey as realized in Table 5, about 108 million tons of waste was generated between the years 2010 through 2018; 94.37% of this consists of ash, slag, BA and gypsum and 70.44% of the waste was sent to ash mountains, ash dams or regular disposal sites. In 2018 alone, 26.1 million tons of waste was generated from 55 thermal PPs and 14 thousand tons of which was classified as hazardous; while 87.5% of the total waste was disposed in ash mountains, ash dams or disposal sites, 12.4% of which was sent to licensed waste treatment facilities and used for backfilling of mines and quarries. Most of the coal waste was disposed in the ash mountains, ash dams or disposal sites URL2, URL3, URL4, URL5, URL6, URL7.

Table 5. Waste statistics of thermal PPs in Turkey.

All running thermal PPs with 100 megawatts (MW) or more		Years				
		2010	2012	2014	2016	2018
The number of thermal power plants		51	59	66	61	55
The amount of non-hazardous waste (ton)		N/A	N/A	24,182,316	19,464,946	26,113,329
The amount of hazardous waste (ton)		N/A	N/A	9,100	11,979	13,805
The amount of total waste (ton)		18,747,759	19,262,185	24,191,416	19,476,925	26,127,134
Disposing (ton)	Disposed in the ash mountains/ash dams	12,186,043	12,982,713	11,684,454	16,224,279	22,861,242
	Landfill	6,561,716	3,679,077	5,249,537		
	Others			3,628,712	3,252,646	26,127
	Sold or sent to licensed waste disposal and recycling companies		2,600,395	3,628,712		3,239,765
N/A: Not available						

The use of BA in concrete rises the compressive strength of concrete as well as the resistance of concrete against abrasion (Aruntaş 2006, Kaplan and Gültekin 2010). Adding 20-30% ash into cement in the construction of concrete roads also reduces the cost of road construction (Kaplan and Gültekin 2010). BA can be partially used in concrete mixtures as a cement substitute, for example this ratio may be 35% or 25% of the cement amount and BA contributes to concrete compressive strength. By using BA, less electrical energy will be used for cement production and so energy savings will be achieved. Since BA is a very thin material, it increases the

workability of concrete as well Arıoğlu and Manzak (1992). The Ministry of Environment and Urbanization of Turkey states that in accordance with the general technical specification for construction, there should be a minimum of 250 kg/m^3 cement and 50 kg/m^3 BA to be used in the roller compacted concrete mixture. Additionally, according to the general technical specifications for RC works, it is recommended that mineral additives such as BA should not exceed 30% of the cement amount in order not to deteriorate the permeability property of concrete (Directorate of High Technics Board, 2018). The analyses and unit fees available by the Ministry of Environment and Urbanization of Turkey were used for cost comparisons. For transportation calculations, sand, gravel and cement are brought from the closest mine and factory to the construction site at a distance of 45 km and 164.5 km (Tables 6 and 7). The BA is brought from the Catalagzi Thermal Power Plant at a distance of 12 km (Table 8), which is also assumed that it will be taken free of charge. Table 9 and 10 show the approximate unit costs of one cubic meter of concrete prepared using 100% sand and one cubic meter of concrete prepared using 25% sand and 75% BA, respectively. In the case of using 75% BA in concrete with the current design, the cost comparison is made in Table 11 and the cost comparison between the current design and the more economic design is made in Table 12. The transport formulas (Tables 6-8) were taken from the Ministry of Environment and Urbanization of Turkey. Sand and gravel are brought from Caycuma District that is the closest mine to the construction site, and the density of sand or gravel is taken into account in calculations as 1.6 tons/m^3 to convert ton to m^3.

Table 6. Transportation of 1 m^3 of sand and gravel to the construction site.

Name of analysis: Sand or crushed stone transportation (m^3)					
Item no	Definition	Unit of measure	Quantity	Unit price	Amount ($)
19.100.2495	F = A x K x (0.0007 x M+0.01) x G				4.21
A	Difficulty coefficient		1.00		
G	Density of sand and crushed stone	ton/m^3	1.60		
10.110.1003	K: Motor vehicle carriage coefficient	$	63.33		
M	Transportation distance	km	45.00		
15.100.1002*	Loading, unloading and storing of material.	m^3	0.80	0.563	0.45
*If the material is available on the construction site 80% of the transportation cost will be paid.					
				Transportation and labor cost:	4.66

Table 7. Transportation of 1 ton of cement to the construction site.

Name of analysis: Cement transportation (ton)					
Item no	Definition	Unit of measure	Quantity	Unit price	Amount ($)
19.100.2495	F = A x K x (0.0007 x M+0.01)				7.93
A	Difficulty coefficient		1.00		
10.110.1003	K: Motor vehicle carriage coefficient	$	63.33		
M	Transportation distance	km	164.50		
15.100.1001*	Loading, unloading and stowing of any type of cement	ton	0.50	2.813	1.41
*Half of the unit price will be deducted as the cost of loading at the factory.					
				Transportation and labor cost:	9.33

Table 8. Transportation of 1 m^3 of BA to the construction site.

Name of analysis: BA transportation (m^3)					
Item no	Definition	Unit of measure	Quantity	Unit price	Amount ($)
19.100.2495	F = A x K x (0.0007 x M+0.01) x G				1.63
A	Difficulty coefficient		1.00		
G	Density of BA	ton/m^3	1.40		
10.110.1003	K: Motor vehicle carriage coefficient	$	63.33		
M	Transportation distance	km	12.00		
15.100.1002*	Loading, unloading and storing of material.	m^3	0.80	0.5633	0.45
*Eighty percent of the unit price will be paid as no storing at the construction site					
				Transportation and labor cost:	2.08

Cement is brought from city of Bolu that is the closest cement factory to the construction site and the density of cement is not taken into account in the calculation because no conversion is needed. BA is brought from Catalagzi Thermal Power Plant and the density of BA is taken into account in calculations as 1.4 tons/m^3.

Unit prices of plant-mixed concrete in Tables 9 and 10 were calculated using the construction unit prices and analyses of the Ministry of Environment and Urbanization of Turkey. The calculated unit prices show approximate market prices and may vary.

In the case of the current design shown in Table 11, a price comparison was made when using 100% sand and using 25% sand-75% BA in ready-mixed concrete. The difference is not significant when the cost of disposal and pollution to nature are not considered. The difference is occurred from that the BA is assumed to be taken free of charge, and the transportation distance is approximately one quarter of the sand transportation distance.

It is seen in Table 12 that the difference increases significantly when 75% of the BA is used in the calculation when considering the mechanical properties of the BA.

Table 9. Unit price of 1m^3 of C25/30 plant-mixed concrete with 100% sand.

Item no	Definition	Unit of measure	Quantity	Unit price	Amount ($)
	Material (C25/30 cement mortar):				
10.130.1026	Sand	m^3	0.5000	4.27	2.14
	Sand transportation	m^3	0.5000	4.66	2.33
10.130.1029	Crushed stone (up to 32 mm)	m^3	0.7100	6.56	4.66
	Crushed stone transportation	m^3	0.7100	4.66	3.31
10.130.1204	Portland cement (bulk)	ton	0.3750	38.67	14.50
	Portland cement transportation	ton	0.3750	9.33	3.50
10.130.9991	Water	m^3	0.1550	1.47	0.23
	Labor:				
	Pumping and pouring:				
19.100.1059	Automatic concrete plant (1000 L capacity, 50 m3/hour) hourly rate	h	0.0200	7.55	0.15
10.100.1015	Concrete master	h	0.3000	3.08	0.92
10.100.1063	Expert laborer	h	0.3000	2.40	0.72
10.100.1051	Driver	h	0.6000	3.13	1.88
10.100.1055	Machine operator	h	0.6000	3.61	2.17
10.100.1057	Assistant operator	h	0.6000	2.96	1.78
10.160.1026	Diesel fuel	kg	1.4250	1.08	1.54
10.160.1030	Electric power	kWh	8.7500	0.13	1.11
10.100.1062	Unskilled construction worker	h	5.0000	2.25	11.25
	Compacting and protecting:				
19.100.1033	Concrete vibrator hourly rate	h	0.3125	4.88	1.52
10.130.9991	Water (for curing)	m^3	0.5000	1.47	0.73
10.100.1015	Concrete master	h	0.9375	3.08	2.88
	Sampling and laboratory tests:				
10.100.1060	Foreman	h	0.3125	4.52	1.41
10.100.1062	Unskilled construction worker	h	0.3125	2.25	0.70
				Material and labor cost:	59.42
				25% contractor's profit and overheads:	14.86
				Price per m^3:	74.28

Table 10. Unit price of 1m³ of C25/30 plant-mixed concrete with 25% sand and 75% BA.

Item no	Definition	Unit of measure	Quantity	Unit price	Amount ($)
	Material (C25/30 cement mortar):				
10.130.1026	Sand	m³	0.5*0.25	4.27	0.53
	Sand transportation	m³	0.5000	0.5*0.25	4.66
N/A	BA (75% substitution for sand)	m³	0.5*0.75	0.00	0.00
	BA transportation	m³	0.7100	0.5*0.75	2.08
10.130.1029	Crushed stone (up to 32 mm)	m³	0.7100	6.56	4.66
	Crushed stone transportation	m³	0.7100	0.7100	4.66
10.130.1204	Portland cement (bulk)	ton	0.3750	38.67	14.50
	Portland cement transportation	ton	0.3750	0.3750	9.33
10.130.9991	Water	m³	0.1550	1.47	0.23
	Labor:				
	Pumping and pouring:				
19.100.1059	Automatic concrete plant (1000 L capacity, 50 m3/hour) hourly rate	h	0.0200	7.55	0.15
10.100.1015	Concrete master	h	0.3000	3.08	0.92
10.100.1063	Expert laborer	h	0.3000	2.40	0.72
10.100.1051	Driver	h	0.6000	3.13	1.88
10.100.1055	Machine operator	h	0.6000	3.61	2.17
10.100.1057	Assistant operator	h	0.6000	2.96	1.78
10.160.1026	Diesel fuel	kg	1.4250	1.08	1.54
10.160.1030	Electric power	kWh	8.7500	0.13	1.11
10.100.1062	Unskilled construction worker	h	5.0000	2.25	11.25
	Compacting and protecting:				
19.100.1033	Concrete vibrator hourly rate	h	0.3125	4.88	1.52
10.130.9991	Water (for curing)	m³	0.5000	1.47	0.73
10.100.1015	Concrete master	h	0.9375	3.08	2.88
	Sampling and laboratory tests:				
10.100.1060	Foreman	h	0.3125	4.52	1.41
10.100.1062	Unskilled construction worker	h	0.3125	2.25	0.70
				Material and labor cost:	56.86
				25% contractor's profit and overheads:	14.21
				Price per m³:	71.07

Table 11. Cost comparison in case of using 75% BA in concrete with the current design.

Type	Section		Total length	Concrete volume	Concrete with 100% sand	Concrete with 75% BA
	m	m	m	m³	($/m³)	($/m³)
Column	0.60	0.60	486.00	174.960		
Column	0.70	0.70	108.00	52.920		
Beam	0.30	0.70	1074.77	225.702		
Beam	0.25	0.70	31.20	5.460	$74.280	$71.071
Beam	0.60	0.70	249.16	104.647		
Beam	0.50	0.70	154.00	53.900		
Beam	0.40	0.70	128.37	35.944		
Total				653.533	$48.544	$46.447
Difference					$2.097	

Table 12. Cost comparison between the current design and the more economic design.

Type	Section		Total length	Concrete volume	Concrete with 75% BA
	m	m	m	m^3	($/$m^3$)
Column	0.35	0.35	486.00	59.535	$71.071
Column	0.40	0.40	108.00	17.280	
Beam	0.25	0.40	635.80	63.580	
Beam	0.25	0.40	31.20	3.120	
Beam	0.30	0.50	238.36	35.754	
Beam	0.30	0.50	141.40	21.210	
Beam	0.30	0.50	103.97	15.596	
Beam	0.40	0.60	442.12	106.109	
Beam	0.40	0.60	33.85	8.124	
Beam	0.40	0.60	10.80	2.592	
			Total	332.899	$23.660
			Difference (48,544-23,660)		$24.884

7. Conclusions

In this study, it has been investigated whether the BA released to the nature as waste material from the thermal power plant can be used in RCSs and how much cost reduction will be caused in construction technology when BA is used in RCSs. In the current design, the cost of concrete used only in beams and columns was calculated as $48,544, and the cost of concrete with 75% BA substitution in concrete was $46,447. The difference was $2,097.

- If the building had been designed considering the mechanical properties of the BA, then the cost difference would have been $24,884. If the foundation of the building is also reanalyzed according to the more economical dimensions, it is obvious that this cost difference will increase even more.
- According to the ready-mixed concrete producers in Zonguldak, it has been stated that approximately 250-300 thousand cubic meters of ready-mixed concrete is used annually in Zonguldak Center, Kozlu and Kilimli Districts. For example, if BA is used in 100 thousand cubic meters of yearly produced ready-mixed concrete, approximately 37,500 cubic meters of BA (100,000*0.375 = 37,500) will be used and the cost difference will be 37,500*($59.42-$56.86) =$96,000.
- Turkey produced 67 million cubic meters of ready-mixed concrete in 2019 according to Turkish Ready-Mixed Concrete Association and according to Turkey Statistical Institute in the year of 2018 data URL2, 22,861,242 cubic meters of coal waste from PPs was disposed. If BA had been used in approximately 10 million cubic meters of concrete, 3.75 million cubic meters of BA would have been used and the cost difference would have been $9,600,000.
- In addition, the use of BA in concrete will significantly reduce the cost of getting rid of the BA and the possible damages to the environment will be prevented.

Acknowledgements

None declared.

Funding

The authors received no financial support for the research, authorship, and/or publication of this manuscript.

Conflict of Interest

The authors declared no potential conflicts of interest with respect to the research, authorship, and/or publication of this manuscript.

References

Albitar M, Visintin P, Mohamed Ali MS, Drechsler M (2015). Assessing Behaviour of fresh and hardened geopolymer concrete mixed with class-F fly ash. *KSCE Journal of Civil Engineering*, 19(5), 1445-1455.

Arıoğlu E, Manzak O (1992). Economic analysis of fly ash use in the construction sector. *Turkey Prefabricated Union*, (22), 25-33.

Aruntaş HY (2006). The potential of fly ash usage in construction sector. *Journal of the Faculty of Engineering and Architecture of Gazi University*, 21(1), 193-203.

Baspinar MS, Demir I, Kahraman E, Gorhan G. (2014). Utilization potential of fly ash together with silica fume in autoclaved aerated concrete production. *KSCE Journal of Civil Engineering*, 18(1), 47-52.

Cao Dz, Selıc E, Hetbell J-D (2008). Utilization of fly ash from coal-fired power plants in China. J*ournal of Zhejiang University Science A*, 9(5), 681-687.

Cavusoglu I, Yilmaz E, Yilmaz AO (2021). Additivity effect on properties of cemented coal fly ash backfill containing water-reducing admixtures. *Construction and Building Materials*, 267, 121021.

Dinelli G, Belz G, Majorana CE, Schrefler BA (1996). Experimental investigation on the use of fly ash for lightweight precast structural elements. *Materials and Structures*, 29, 632-638.

Directorate of High Technics Board (2018). Specifications. Retrieved from https://yfk.csb.gov.tr/sartnameler-i-330.

Dry C, Meier J, Bukowski J (2004). Sintered coal ash/flux materials for building materials. *Materials and Structures*, 37, 114-121.

Esquinas AR, Álvarez JI, Jiménez JR, Fernández JM (2018). Durability of self-compacting concrete made from non-conforming fly ash from coal-fired power plants. *Construction and Building Materials*, 189, 993-1006.

Güler G, Güler E, İpekoğlu Ü, Mordoğan H (2005). Fly ash properties and uses. *Turkey 19th International Mining Congress and Expo*, *IMCET*, İzmir, 419-423.

Huang Q, Li S, Shao Y, Zhao Y, Yao Q (2019). Dynamic evolution of impaction and sticking behaviors of fly ash particle in pulverized coal combustion. *Proceedings of the Combustion Institute*, 37(4), 4419-4426.

Hwang SS, Cortés CMM (2021). Properties of mortar and pervious concrete with co-utilization of coal fly ash and waste glass powder as partial cement replacements. *Construction and Building Materials*, 270, 121415.

Jang HS, Xing S (2020). A model to predict ammonia emission using a modified genetic artificial neural network: Analyzing cement mixed with fly ash from a coal-fired power plant. *Construction and Building Materials*, 230, 117025.

Kaplan G, Gültekin AB (2010). The investigation of fly ash usage in terms of environmental and social effects in construction sector. *International Sustainable Buildings Symposium*, Ankara.

Karalar M (2020). Experimental and numerical investigation on flexural and crack failure of reinforced concrete beams with bottom ash and fly ash. *Iranian Journal of Science and Technology, Transactions of Civil Engineering*, 44(Suppl 1), 331-354.

Karalar M, Bilir T, Çavuşli M (2020). 3D experimental and numerical investigation on crack behaviour of RC beams under %75 bottom ash ratio. *Structures20 Congress*, Korea.

Li T, Sun T, Li D (2018). Preparation, sintering behavior, and expansion performance of ceramsite filter media from dewatered sewage sludge, coal fly ash, and river sediment. *Journal of Material Cycles and Waste Management*, 20, 71-79.

Nakamura K, Inoue Y, Komai T (2021). Consideration of strength development by three-dimensional visualization of porosity distribution in coal fly ash concrete. *Journal of Building Engineering*, 35, 101948.

Ramachandran D, George RP, Vishwakarma V, Mudali UK (2017). Strength and durability studies of fly ash concrete in sea water environments compared with normal and superplasticizer concrete. *KSCE Journal of Civil Engineering*, 21(4), 1282-1290.

SAP2000 (2008). Integrated finite elements analysis and design of structures. Computers and Structures, Inc., Berkeley, CA, USA,

Sönmez G, Işık M (2020). Environmental effects of coal combustion wastes and usage areas. *NOHU Journal of Engineering Sciences*, 9(1), 72-83.

Sun Q, Cai C, Zhang S, Tian S, Li B, Xia Y, Sun Q (2019). Study of localized deformation in geopolymer cemented coal gangue-fly ash backfill based on the digital speckle correlation method. *Construction and Building Materials*, 215, 321-331.

Tan H, Nie K, He X, Deng X, Zhang X, Su Y, Yang J (2019). Compressive strength and hydration of high-volume wet-grinded coalfly ash cementitious materials. *Construction and Building Materials*, 206, 248-260.

URL1: http://www.coal-ash.co.il/docs/BR-111026.pdf.

URL2: https://www.thbb.org/sektor/istatistikler/.

URL3: https://tuikweb.tuik.gov.tr/HbPrint.do?id=10732.

URL4: https://tuikweb.tuik.gov.tr/HbPrint.do?id=16164.

URL5: https://tuikweb.tuik.gov.tr/PreHaberBultenleri.do;jsessionid=15tCfQGGqdtQNBn5sY2JzB3MrdXWQm3YPR4KcHmvrQ1RNCcz90Np!-1175971644?id=18782.

URL6: https://tuikweb.tuik.gov.tr/PreHaberBultenleri.do?id=24873.

URL7: https://tuikweb.tuik.gov.tr/PreHaberBultenleri.do?id=30674.

Verma S, Amritphale SS, Khan MA (2019). Utilization of brine sludge and fly ash waste as complementary resources, for making non-toxic, geopolymeric (cement-free) materials. *Iranian Journal of Science and Technology, Transactions of Civil Engineering*, 43(Suppl 1), 603-614.

Wang L, Sun H, Sun Z, Ma E (2016). New technology and application of brick making with coal fly ash. *Journal of Material Cycles and Waste Management*, 18, 763-770.

Wu T, Chi M, Huang R (2014). Characteristics of CFBC fly ash and properties of cement-based composites with CFBC fly ash and coal-fired fly ash. *Construction and Building Materials*, 66, 172-180.

Yost JR, Radlin´ska A, Ernst E, Salera M (2013). Structural behavior of alkali activated fly ash concrete. Part 1: mixture design, material properties and sample fabrication. *Materials and Structures*, 46, 435-447.

Challenge Journal of Concrete Research Letters

Research Article

Mechanical behavior investigation of rubberized concrete barriers in impact load

Hasan Selim Şengel [a,*], Ahmet Şahin Özgören [a], Hakan Erol [a], Mehmet Canbaz [a]

[a] *Department of Civil Engineering, Eskişehir Osmangazi University, 26480 Eskişehir, Turkey*

ABSTRACT

Approximately 1.5 million waste tires are produced annually. Waste tires in landfills and stocks cause toxic chemicals to pollute the soil and cause major fires. Waste tires are a global environmental problem. This problem gave an idea of recycling of waste tires instead of landfills and stocks. In this paper, an experimental study is conducted to review the behavior under impact load of rubberized concrete with conventional concrete. Three different mixes were made by adding crumb rubber (0%, 5% and 10%) by volume to the concrete. Nine cantilever column specimens of three type cross section (10x10, 15x15 and 20x20 cm2) were used to investigate the behavior under impact load. The specimens with higher rubberized concrete have longer impact load duration at the initial peak point. Specimens with rubber content become much flexible than normal specimens. Furthermore, the damage level of columns is greater with increasing rubber content. Therefore, the specimens with higher rubberized concrete absorb more impact energy. The barriers with higher rubber content minimize injury and demise when an accidental impact happens. Using concrete with rubber content reduces costs and produces an environmentally sustainable solution.

ARTICLE INFO

Article history:
Received 27 May 2022
Revised 25 June 2022
Accepted 13 July 2022

Keywords:
Waste tire
Impact load
Rubberized concrete
Reinforced barrier

1. Introduction

Parallel to the quickly increasing traffic opportunities and traffic demand global in the last hundred years; because of traffic accidents, financial and health losses are rapidly increasing day by day, so, leading scientists to take some preventions to resolve the issue. One of these preventions is the roadside concrete barrier, which is expressed as a wayside security (Apak et al. 2021). Wayside security is one of the significant topic of highway systems due to its important ratio of high-seriousness accident. Roadside rigid barriers have an important role in decreasing the collision severity and rescuing more people on highway but prefer an unsuitable roadside barrier could reduce roadside barriers' performance (Molan et al. 2018). Therefore, researchers are researching for barriers that will reduce the impact load in accidents.

Collection of waste tire is later increased to dangerous grades. Tire waste is one of them that create significant ecological issues because of the increment and many variations of modern universal. Therefore, recycling waste tire rubber in the form of aggregates as complementary structure material is beneficial (Siddika 2019). In addition, waste tires cause important health and ecological pollution if not recycled. More and more, recycling waste tires into structure engineering utilizations, especially into concrete, has been wining interests (Shu 2013). Thus, this problem gave an idea of recycling of waste tires instead of landfills and stocks.

Behavior under static load of rubberized concrete with conventional concrete has been tested by many researchers. According to Youssf et al. (2015) crumbed rubber in the concrete beam improved the hysteretic damping ratio and energy dissipation by 13% and 150%. On the other hand, it reduced the column viscous damping ratio by 49% checked to a normal concrete column. Alasmari et al. 2019 investigated the mechanical properties of conventional beams with rubberized hybrid beams. The experimental results determined develop-

* *Corresponding author*. Tel.: +90-222-239-3750 ; Fax: +90-222-229-0535 ; E-mail address: ssengel@ogu.edu.tr (H. S. Şengel)
ISSN: 2548-0928 / DOI: https://doi.org/10.20528/cjcrl.2022.03.002

ments when the hybrid concrete beams were used in most cases such as collapse pattern, capacity load, ductility, stiffness and stress. The deflection capacity of rubberized concrete beams with conventional concrete beams have been researched by Hassanli et al. (2017). The experimental result found that an increment from 7.7% to 27.9% was determined in the deflection capacity of the rubberized concrete beam checked with the beam with conventional concrete beam. According to Vadivel et al. (2010) the flexural strength comparison in both the grades (M20 and M25) indicate that 2%, 4% and 6% replacements behave exceptionally well and show higher strength than the conventional concrete.

On the other hand, other studies focused on the mechanical properties of rubberized concrete with conventional concrete in impact load. A study by Al-Tayeb et al. (2013) investigated mechanical behavior of rubberized concrete in static, dynamic and impact load by compare. The bending load-flexibility attitude was examined for the conventional and hybrid beams (double layer beam with rubberized (10% and 20% replacements by volume) top and normal bottom), under static and impact loads. Specimens (size 50 mm _ 100 mm _ 400 mm) were loaded to collapse in a drop-mass impact vehicle by dropping a 20 N mass from elevation 300 mm to the center of a simply supported specimen, and the static load test were performed with same beams. The using of crumbed rubber in concrete beam increases flexural impact feature of the specimen while dynamic loading crosschecked to the static loading. In addition the adding of crumbed rubber increased the toughness and flexibility capability of the conventional beam. The effect of maximum impact force and impact duration of rubberized concrete with conventional concrete in accident, have been researched by Pham et al. (2018). The outcome of experiment have shown that rubberized concrete quite decreased the capacity impact force of up to 50% and increased the impact time. These features make crumbed rubber in concrete an encouraging materiel for safety construction and especially for future structures of inflexible roadside barriers. Crumbed rubber in concrete decreased the capacity impact force so that it delivered a lower force to roadside barriers as well as a lower rebound force, which is desirable for conservation of voyagers in an accident. According to Abdelmonem et al. (2019) an obvious decrease of approximately up to 50% in compressive, tensile, and flexural strength was detected with increasing the crumbed rubber up to 30%. The crumbed rubber in concrete beam mixes displayed great attitude in salt water. The rubberized concrete also had up to 83% higher impact durability checked to the conventional concrete.

The above studies concluded that rubberized concrete has higher energy absorption, hysteretic damping ratio, impact duration, toughness, deformation ability, and good behavior in seawater but lower compressive, tensile and flexural strength, maximum impact force viscous damping ratio than the corresponding conventional concrete.

The review of literature reveals that there has been no work carried out on rubberized cantilever concrete under impact loading. Therefore, in this paper an experimental study is conducted to review the behavior under impact load of rubberized concrete cantilever column with conventional concrete.

2. Experimental Study

2.1. Materials

Three types of rubberized concrete mixed (%0, %5 and %10) were used in casting concrete barrier specimens. The conventional concrete had the compressive strength of 30 MPa. The crumb rubber was manufactured by waste tire. Crumb rubber added to the concrete mix are shown in Fig 1. Rubber at 5% and 10% were added to mix of the rubberized concrete. All the collected experimental result were gained with the help of LabView SignalExpress program by National Instruments throughout the experimental study. Moreover all the collected data refined with the help of DIAdem program by National Instruments.

Fig. 1. 2-3 mm diameter crumbed rubber.

2.2. Method and tests

2.2.1. Test specimens

Table 1 shows the test specimens and their properties used in this study. A total of 9 specimens with three types of cross-section area (10x10, 15x15 and 20x20 cm^2) were produced. 0.5% percentage reinforcement was placed in the tension zone of the cantilever specimen. Three concrete mixes (conventional concrete, 5% rubber concrete and 10% rubber concrete) were planned to investigate the effects of the amount of rubberized concrete. Fig. 2 shows the production of specimens in the laboratory.

2.2.2. Experimental setup and procedure

Fig. 3 displays the drop weight machine, which was produced to examine the impact load test of specimen. After the weight used for the impact test is released, it moves on the rails and falls on the specimen. In this study, experiments were carried out for all samples with 84 kg impact load and 40 cm drop height. Fig. 3 shows

the accelerometers and load cell. Two accelerometers were placed on the right and left side surfaces of the cantilever specimen. The load cell with plates was placed on the upper surface of the cantilever sample. Fig. 3 shows the support assembly of the experimental setup. The specimen was supported from two points using plates and anchors. These two supports caused the reinforced concrete specimen to act as a cantilever.

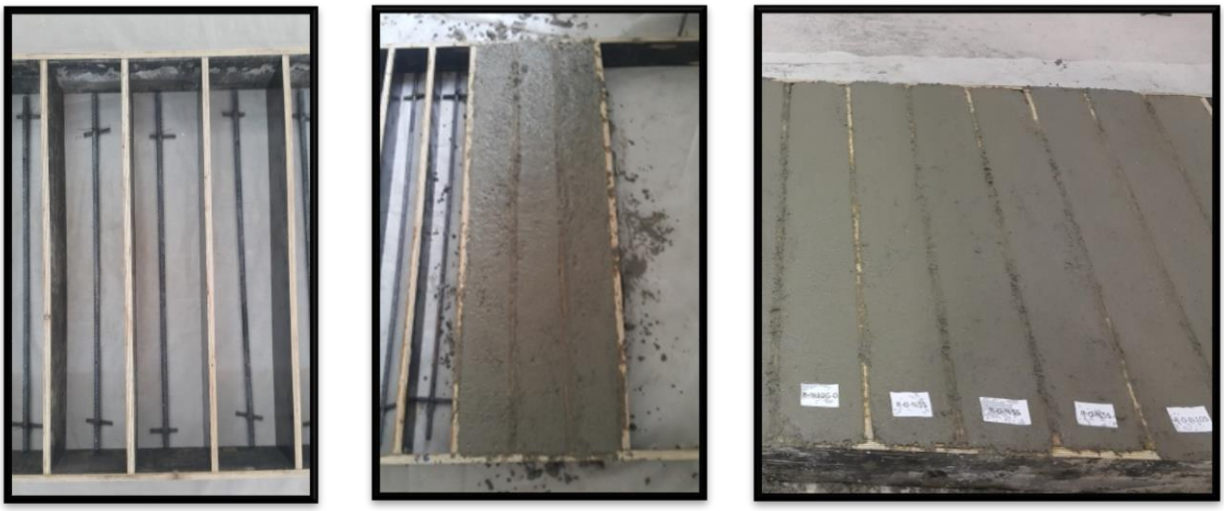

Fig. 2. Production of specimens in the laboratory.

Fig. 3. Experimental setup.

Table 1. Test specimens.

Specimen	Cross-section	Length	Rubber ratio	Concrete	Percentage
C10x10x110R-0G	10X10 cm²	110 cm	0%	C30	%0.5
C10x10x110R-5G	10X10 cm²	110 cm	5%	C30	%0.5
C10x10x110R-10G	10X10 cm²	110 cm	10%	C30	%0.5
C15x15x110R-0G	15X15 cm²	110 cm	0%	C30	%0.5
C15x15x110R-5G	15X15 cm²	110 cm	5%	C30	%0.5
C15x15x110R-10G	15X15 cm²	110 cm	10%	C30	%0.5
C20x20x110R-0G	20X20 cm²	110 cm	0%	C30	%0.5
C20x20x110R-5G	20X20 cm²	110 cm	5%	C30	%0.5
C20x20x110R-10G	20X20 cm²	110 cm	10%	C30	%0.5

3. Discussion

3.1. Time-impact force histories

The time impact load histories read by the load cell on the concrete column surface is shown in Fig. 2. All the charts of concrete specimens show a parallel pattern with the first maximum point. First maximum impact force was quite more than next peaks. There is a space between the initial and next impact force with negative impact force. The meaning of this gap is the separation of the connection between the column and the impactor. First peak impact force time is shown in Fig. 4.

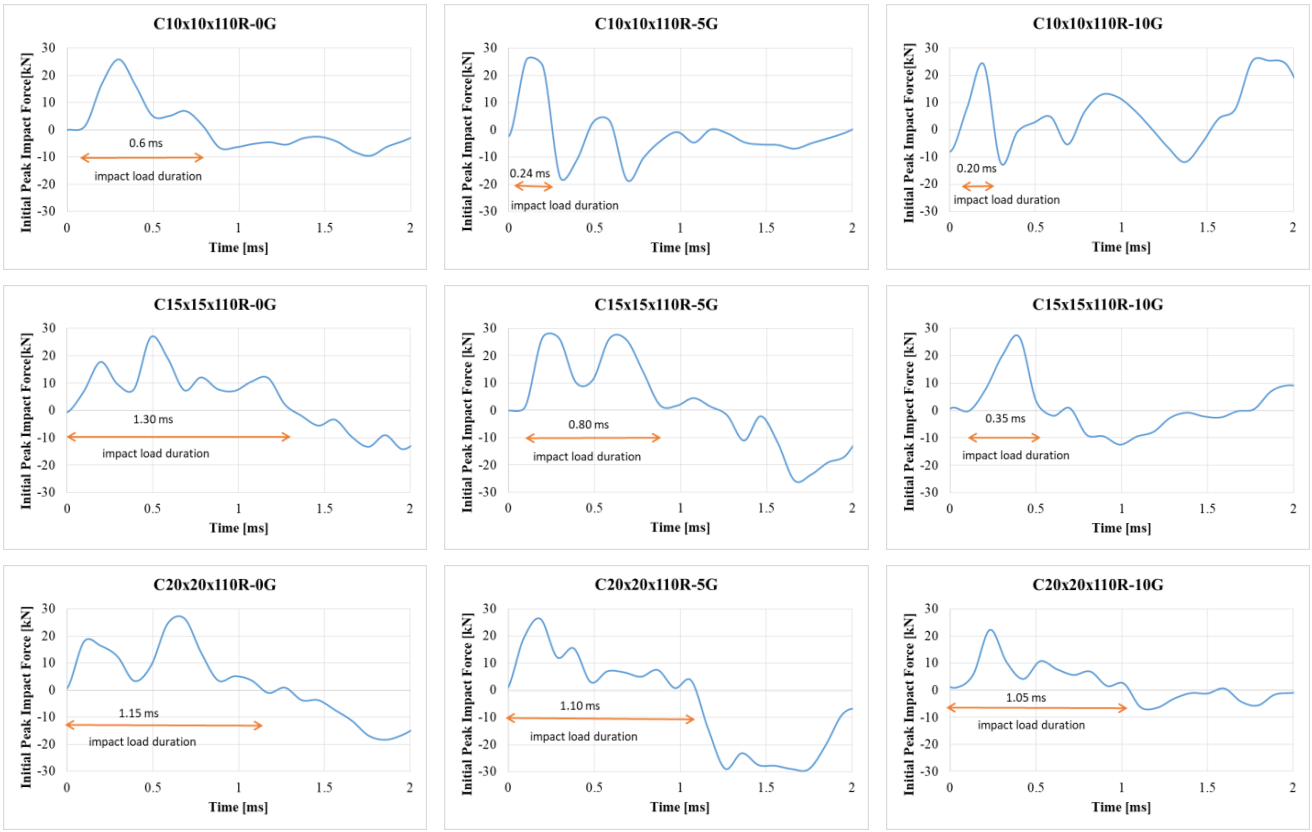

Fig. 4. Initial maximum impact force time.

The impact load time at the initial maximum point is about 0.60 ms for the normal concrete column C10x10x110R-0G, 0.24 ms for the %5 rubberized concrete column C10x10x110R-5G and 0.20 ms for the %10 rubberized concrete column C10x10x110R-10G. %5 and %10 rubberized concrete columns' impact load duration decreased %60 and %67 respectively. As a result, the columns with higher rubber content have longer impact load time at the initial peak point. On the other hand as seen in the graphs, for the other cross sections, the increase in the rubber amount shows a similar effect. It is advantageous to use rubber in con-

crete barriers due to the shortening of the impact load time at the initial peak point. Therefore, the barriers with higher rubber content minimize injury and demise when an accidental impact happens. Impact load time histories of the analyzed specimens are displayed in Fig. 5.

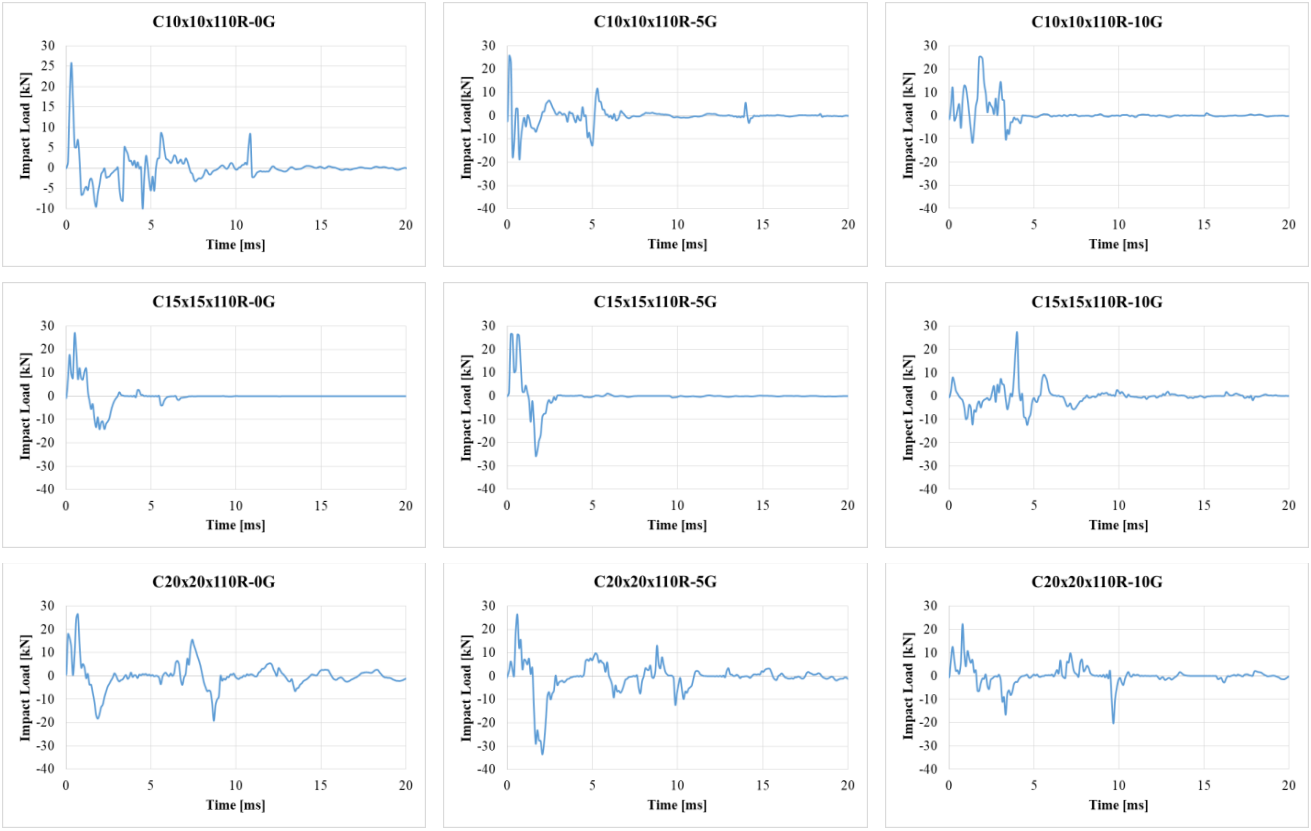

Fig. 5. Impact load-time histories of the tested beams.

3.2. Time-deformation histories

The time deformation histories of the specimens were produced from LVDT at the tracking points from the column end as shown in Fig. 5. In addition, the maximum displacement and residual displacement at the end of the column are presented in Figs. 6 and 7. Maximal deformation of columns of 20x20 cross section under impact load is quite small and most of this deformation is in the elastic region. As the cross section decreased, the maximum displacement and residual displacement increase and most of this deformation is in the plastic region. Maximum deformation - Rubber Ratio of the beams in the impact load are shown in Fig. 6. Residual deformation - rubber ratio of the beams in the impact load are shown in Fig. 7.

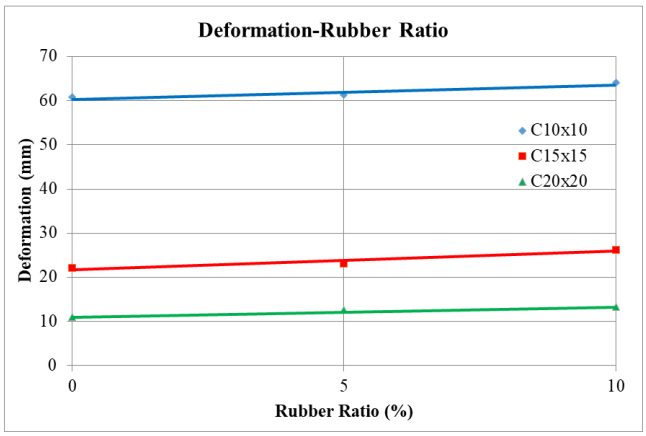

Fig. 6. Maximum deformation - rubber ratio of the beams in the impact load.

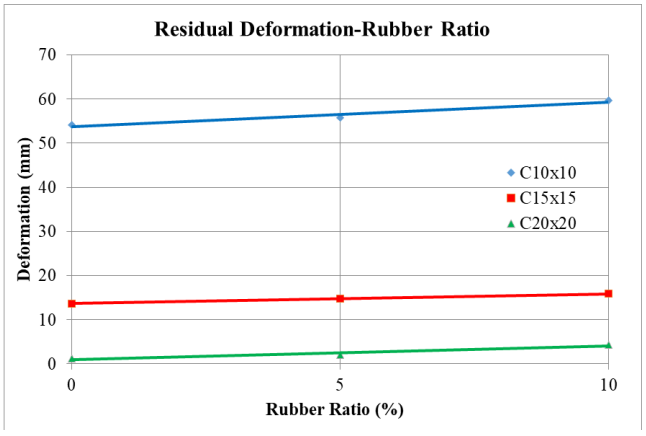

Fig. 7. Residual deformation - rubber ratio of the beams in the impact load.

The maximal deformation at the impact point of conventional columns (for cross sections 10x10,15x15 and 20x20 respectively) was 60.7-22.1-10.8 mm while the corresponding values of the specimens with 5% and 10% rubberized concrete were 61.1-23.1-12.5 mm, and 63.9-26.3-13.1 mm.

These results show that rubberized concrete columns become much more flexible than normal concrete columns. In addition, as the column cross-section gets larger the effect of the rubber on the deformation increases. Displacement time histories of the analyzed specimens are displayed in Fig. 8.

3.3. Time-acceleration histories

Acceleration time histories of the analyzed specimens are displayed in Fig. 9. Maximum average acceleration–rubber ratio of the beams in the impact load are shown in Fig. 10.

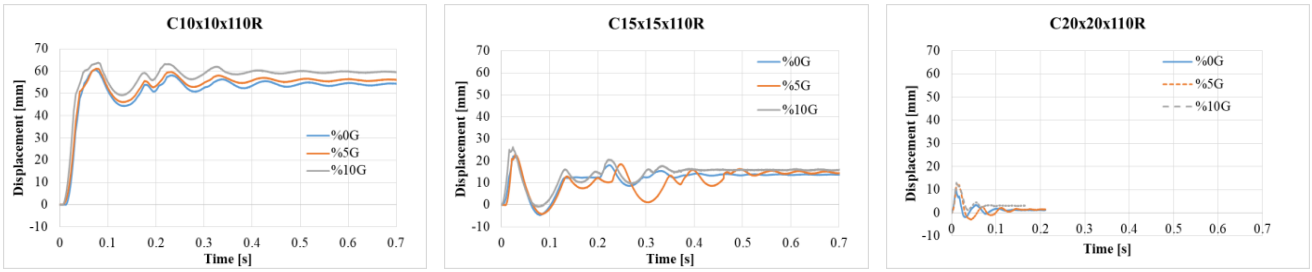

Fig. 8. Displacement-time histories of the tested beams.

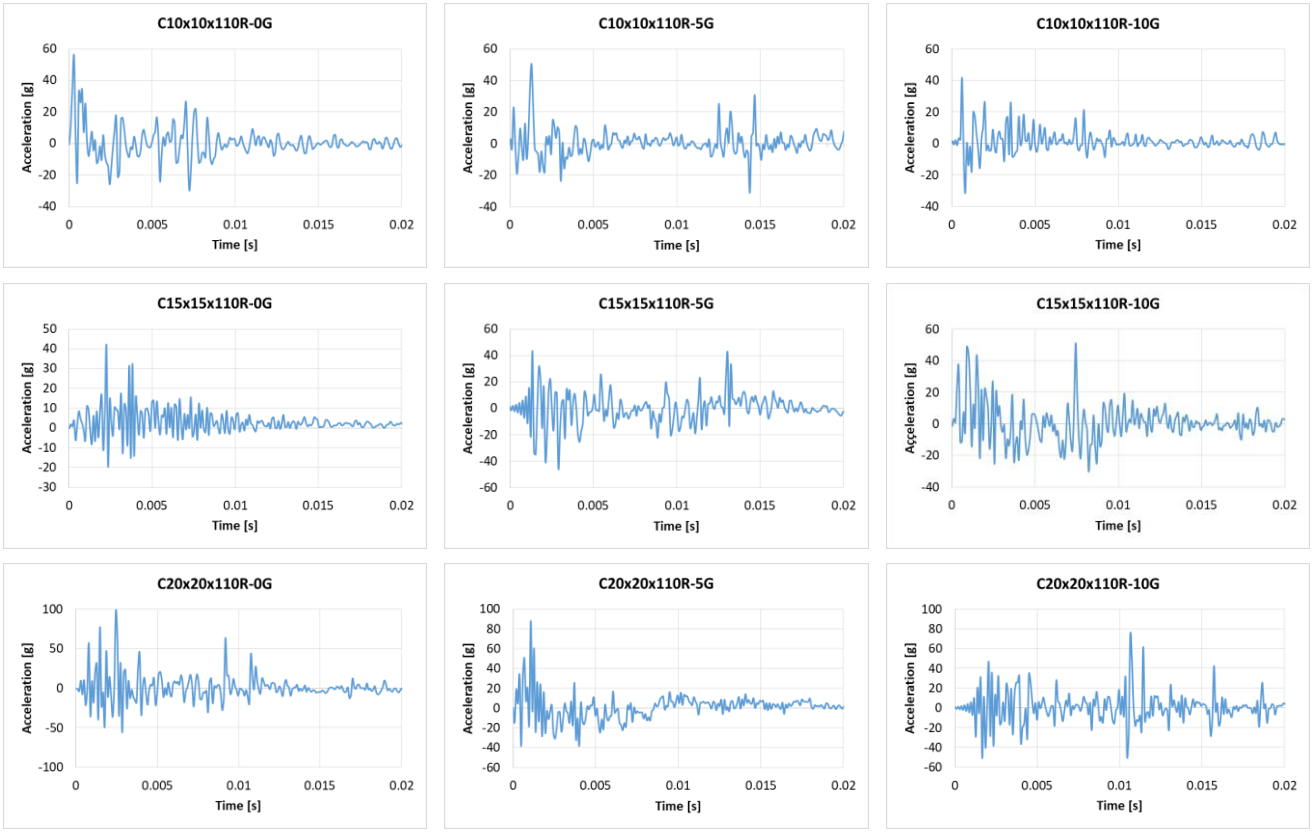

Fig. 9. Acceleration-time histories of the tested beams.

3.4. Deformation and progressive failure

The behavior of columns under impact loading consists of two phase. The first phase is the impact force phase, where the impactor transfers the load to the column. In this study, the first phase consists of about 10ms-20ms. The other phase is the free vibration phase which the impactor has no connection with the column. The second stage consists of about 1s.

Table 1 shows impact failure of cantilever column C10x10x110R-0G, C10x10x110R-5G and C10x10x110R under Impact load. The failure of columns with different rubber content were investigated. The damage level of columns is greater with increasing rubber content therefore, the columns with higher rubber content absorb more impact energy. Impact failure of cantilever column C10x10x110R-0G, C10x10x110R-5G and C10x10x110R in impact load are shown in Fig. 11.

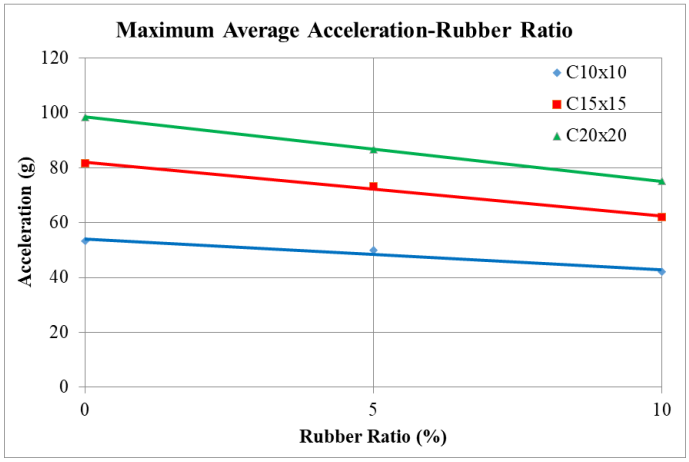

Fig. 10. Maximum average acceleration - rubber ratio of the beams in the impact load.

Fig. 11. Impact failure of cantilever column C10x10x110R-0G, C10x10x110R-5G and C10x10x110R in impact load.

4. Conclusions

In this paper, an experimental study is conducted to review the behavior under impact load of rubberized concrete cantilever column with conventional concrete.

The findings can be summarized as follows:

- The damage level of columns is greater with increasing rubber content therefore, the maximum rubberized concrete column content absorb more impact energy.
- Rubberized concrete columns become much flexible than normal concrete columns.
- The barriers with higher rubber content minimize injury and demise when an accidental impact happens.
- The maximum rubberized concrete columns have longer impact load duration at the initial peak point.
- 5% and 10% rubberized concrete columns' impact load duration decreased 60% and 67% respectively in C10x10x110R.
- Under the impact energy, rubberized concrete has slightly much deformation relative to conventional concrete.
- %5 and %10 rubberized concrete columns' residual deformation increased 64% and 242% respectively in C20x20x110R.
- The use of concrete with rubber content reduces costs and produces an environmentally solution.

Waste tires in landfills and stocks cause toxic chemicals to pollute the soil and cause major fires. Waste tires are a global environmental problem. This experimental study investigated the effect of steel wires recycled waste tire on concrete properties. Rubberized concrete columns become much flexible than normal concrete columns. Therefore, the barriers with higher rubber content minimize injury and demise when an accidental impact happens. As a result, the use of waste tire in reinforced concrete building elements should be expanded. Waste tire recycling is important for a sustainable environment and traffic safety.

Acknowledgements

None declared.

Funding

The authors received no financial support for the research, authorship, and/or publication of this manuscript.

Conflict of Interest

The authors declared no potential conflicts of interest with respect to the research, authorship, and/or publication of this manuscript.

REFERENCES

Abdelmonem A, El-Feky MS, Nasr EAR, Kohail M (2019). Performance of high strength concrete containing recycled rubber. *Construction and Building Materials,* 227, 116660.

Alasmari HA, Bakar BH, Noaman AT (2019). A comparative study on the flexural behavior of rubberized and hybrid rubberized reinforced concrete beam. *Civil Engineering Journal,* 5(5), 1052-1067.

Al-Tayeb MM, Bakar BHA, Ismail H, Akil HM (2013). Effect of partial replacement of sand by recycled fine crumb rubber on the performance of hybrid rubberized-normal concrete under impact load: experiment and simulation. *Journal of Cleaner Production*, 59, 284–289.

Apak MY, Yumrutaş Hİ (2021). An evaluation on measuring bollard performance experimentally on urban roadside safety. 3rd *International Symposium of Engineering Applications on Civil Engineering and Earth Sciences*.

Hassanli R, Youssf O, Mills JE (2017). Experimental investigations of reinforced rubberized concrete structural members. *Journal of Building Engineering*, 10, 149-165.

Molan AM, Ksaibati K (2018). Developing the new barrier condition index to unify the barrier assessments – a case study in Wind River Indian reservation, Wyoming. *The Open Transformation Journal*, 12, 182-191.

Pham TM, Zhang X, Elchalakani M, Karrech A, Hao H, Ryan A (2018). Dynamic response of rubberized concrete columns with and without FRP confinement subjected to lateral impact. *Construction and Building Materials,* 186, 207-218.

Shu X, Huang B (2014). Recycling of waste tire rubber in asphalt and portland cement concrete: An overview. *Construction and Building Materials*, 67, 217–224.

Siddika A, Mamun AA, Alyousef R, Amran YHM, Aslani F, Alabduljabbar H (2019). Properties and utilizations of waste tire rubber in concrete: A review. *Construction and Building Materials*, 224, 711-731.

Vadivel TS, Thenmozhi R (2010). Characteristic study on rubbercrete-an innovative construction material produced through waste tyre rubber. *Manager's Journal on Civil Engineering*, 1(1), 34-39.

Youssf O, ElGawady MA, Mills JE (2015). Experimental investigation of crumb rubber concrete columns under seismic loading. *Structures*, 3, 13-27.

Challenge Journal of Concrete Research Letters

Research Article

Effect of waste concrete powder on slag-based sustainable geopolymer composite mortars

Erdinç Halis Alakara [a], Özer Sevim [b,*], İlhami Demir [b], Gazi Günel [c]

[a] *Department of Civil Engineering, Tokat Gaziosmanpasa University, 60150 Tokat, Turkey*
[b] *Department of Civil Engineering, Kırıkkale University, 71451 Kırıkkale, Turkey*
[c] *Graduate School of Natural Applied Sciences, Kırıkkale University, 71451 Kırıkkale, Turkey*

ABSTRACT

In this study, the effect of waste concrete powder (WCP) on slag-based geopolymer composite mortars was investigated. Blast furnace slag (BFS) and WCP were used as binders in geopolymer mortars. WCP was substituted into the geopolymer mortar composites at rates of 10%, 20%, 30%, and 40% by weight of slag. Sodium hydroxide (NaOH) solution was used as the alkali activator in the mixtures and the solution activator concentration was chosen as 16 molars (M). After the prepared mortars were cured at 100°C for 24 hours, they were subjected to flexural strength (f_{fs}), compressive strength (f_{cs}), and ultrasonic pulse velocity (UPV) tests. Results showed that f_{fs}, f_{cs}, and UPV decreased with the increase in WCP replacement ratio. These decrements were seen clearly, especially after the 20% replacement ratio. However, despite these decrements, the compressive strengths of all groups were found to be above 50 MPa. In addition, it is thought that environmental pollution can be reduced by using WCP in geopolymer composite mortars.

ARTICLE INFO

Article history:
Received 7 August 2022
Revised 22 August 2022
Accepted 14 September 2022

Keywords:
Waste concrete powder
Geopolymer composite mortars
Alkali-activated slag
Compressive strength
Flexural strength
Ultrasonic pulse velocity

1. Introduction

The developments in concrete technology and the rapid increase in the global population have also increased housing needs. As a result of this situation, ordinary Portland cement (OPC) has become the world's most widely used construction material. A high number of raw materials and energy are consumed during the production of OPC (Li et al. 2019; Tahwia et al. 2022, Toklu 2021). It is also stated that OPC production is responsible for 7% of the world's greenhouse gas emissions (Meyer 2009; Sevim and Sengul 2021; Toklu and Şimşek 2018). These reasons have led researchers to work on developing more environmentally friendly and alternative binders to OPC (Sahmaran et al. 2013; Mehta and Siddique 2017; Demir et al. 2018; Sevim and Demir 2019). Developed as an alternative to OPC, geopolymer binders have been studied with increasing interest in recent years, as they consume less energy and emit less CO2 compared to OPC (Provis 2014; Geraldo et al. 2017; Alhawat et al. 2022).

It has been stated that geopolymers have many advantages such as superior mechanical properties (Mahmoodi et al. 2022), high resistance to elevated temperature (Çelikten et al. 2020), acid (Thokchom et al. 2009), and sulfate effects (Bhutta et al. 2013), as well as environmentally friendly properties. Geopolymers are produced as a result of the chemical reaction between aluminosilicate sources (precursors) such as metakaolin, blast furnace slag (BFS), fly ash (FA), and alkaline activators such as NaOH, Na_2SiO_3 (Rakhimova 2020; Öztürk and Atabey 2022). These aluminosilicate sources, widely used in geopolymers' production, were formerly seen as industrial by-products or waste. However, these products are no longer considered waste due to their successful and widespread use for years (Ulugöl et al. 2021). This situation has led researchers to investigate the use of different waste materials in geopolymer composites (Shoaei et al. 2019; Mahmoodi et al. 2021a).

Construction and demolition waste (CDW), which is responsible for most of the global solid waste production,

* *Corresponding author*. Tel.: +90-318-357-4242/1263 ; E-mail address: ozersevim@kku.edu.tr (Ö. Sevim)
ISSN: 2548-0928 / DOI: https://doi.org/10.20528/cjcrl.2022.03.003

has become a rapidly growing problem worldwide. While the 28 member countries of the European Union produced approximately 1.65 tons of CDW per capita in 2012, the United States of America produced approximately 1.7 tons of CDW per capita in 2015 (Ulugöl et al. 2021). Uncontrollable CDW production will continue to threaten the health of living things and the environment day by day (Wang et al. 2014). Geopolymers have been produced using some CDW products (concrete, glass, tiles, bricks, etc.).

Öztürk and Atabey (2022) produced geopolymer mortars containing recycled ceramic sanitaryware waste powder (CSW). NaOH as alkali activators in four different molars (10, 12, 14, and 16 M) and two different water/binder (w/b) ratios (0.45 and 0.50) were used in the mixtures. The increase in NaOH concentration increased the workability of the CSW-added mortars while decreasing their porosity and water absorption. The highest strength values were obtained from geopolymer mortars produced with 16 M NaOH and a 0.45 w/b ratio. Ahmari et al. (2012) investigated the combined use of waste concrete powder and F class FA as geopolymeric binders. The results showed that no significant improvement in compressive strength was achieved with the use of waste concrete powder alone, while there was an increase in compressive strength when used together with F class FA. Tahwia et al. (2022) produced ultra-high performance geopolymer concrete by using crushed glass (CG), ceramic (CC) and crumb rubber (CR) wastes as aggregates in geopolymer mortars. According to the results, it was observed that the mechanical and microstructural properties of the mixtures decreased significantly with the inclusion of CC and CR and increased with the inclusion of CG. A denser microstructure was obtained by incorporating CG into the mixtures.

In this study, the effect of waste concrete powder (WCP) on slag-based geopolymer composite mortars was investigated. Blast furnace slag (BFS) and WCP were used as binders in geopolymer mortars. WCP was substituted into the geopolymer mortar composites at rates of 10, 20, 30, and 40% by weight of slag. Sodium hydroxide (NaOH) solution was used as the alkali activator in the mixtures and the solution activator concentration was chosen as 16 molars (M). After the prepared mortars were cured at 100°C for 24 hours, they were subjected to flexural strength (f_{fs}), compressive strength (f_{cs}), and ultrasonic pulse velocity (UPV) tests. Finally, the obtained results were compared with control geopolymer mortars without waste concrete powder replacement.

2. Materials and Method

In the preparation of geopolymer mortars, standard sand defined by CEN (Committee of European Norms) in TS EN 196-1 was used. The sand was obtained from the local source in Turkey. BFS was selected according to ASTM C989 (ASTM 2014b). WCP was obtained by grinding the materials collected from the landfill. The ground material was used after sieving through the 75 μm sieve. The chemical oxide composition and physical properties of BFS and WCP are given in Table 1. NaOH in the form of white pellets with a purity of about 99% was used as an alkali activator in the mixtures.

Table 1. Chemical oxide composition and physical properties of BFS and WCP.

Chemical composition (%)	BFS	WCP
SiO_2	35.97	26.38
Al_2O_3	16.05	5.23
Fe_2O_3	0.66	2.06
MgO	5.43	9.45
CaO	37.38	32.96
Na_2O	0.38	0.51
K_2O	0.81	0.75
TiO_2	0.58	0.23
Physical properties		
Relative density (g/cm³)	3.06	2.69
Loss on ignition (LOI)	1.18	21.98

Mixing ratios of geopolymer mortars are given in Table 2. Fresh geopolymer mortars prepared per TS EN 196-1 were filled in molds with dimensions of 40×40×160 mm in two stages and compressed on the shaking table. It was then cured in an oven at 100°C for 24 hours. Ultrasonic pulse velocity (UPV) test was conducted per ASTM C 597-16 standard for the geopolymer mortars whose curing process was completed. Table 3 shows the classification of the quality of concrete as a function of the ultrasonic pulse velocity (Whitehurst 1951; Qasrawi 2000). Afterward, the flexural strengths of the samples were determined per TS EN 196-1. In addition, the compressive strength test was conducted on the broken parts of the prismatic samples after the flexural strength test.

Table 2. Mixing ratios of geopolymer mortars.

Mixture Code	BFS (g)	WCP (g)	WCP ratio (%)	Water (g)	Sand (g)	NaOH (g)	Molarity (M)	Curing time (hour)	Curing temperature (°C)
Ref	450	0	0						
WCP10	405	45	10						
WCP20	360	90	20	192.60	1350	144	16	24	100
WCP30	315	135	30						
WCP40	270	180	40						

Table 3. Quality of concrete as a function of the ultrasonic pulse velocity (Whitehurst 1951).

UPV (km/h)	>4.5	3.5–4.5	3.0–3.5	2.0–3.0	<2.0
Quality	Excellent	Good	Doubtful	Poor	Very poor

3. Results and Discussion

3.1. Flexural strength (f_{fs})

The f_{fs} test results performed per the TS EN 196-1 standard are shown in Fig. 1(a). For the mixtures with each code, the average of the results of three samples was taken as the final f_{fs} results. The percentage of decrease in f_{fs} results of slag-based geopolymer mortars incorporating WCP compared to control geopolymer mortars without WCP is shown in Fig. 1(b).

When the f_{fs} results given in Fig. 1 are examined, it is seen that the f_{fs} results vary between 12.05 and 10.45 MPa. The f_{fs} results of the WCP10, WCP20, WCP30, and WCP40 decreased by 2.84, 4.07, 7.80, and 13.27%, respectively, compared to the Ref mortars. The rate of decrease in f_{fs} results increased with the increase of the WCP replacement ratio. BFS particles provide the formation of calcium alumina silicate hydrate (C-A-S-H) and/or calcium silicate hydrates in the geopolymeric gel system (Rakhimova and Rakhimov 2015; Mahmoodi et al. 2021b). As the amount of WCP in the mixtures increases, the amount of BFS decreases. As a result of this situation, the hydrated element density in the matrix of geopolymer mortars decreases. Tan et al. (2020) stated in their study that the geopolymer samples became much denser with the addition of BFS. These conditions can be shown as the reason for the decrease in f_{fs} results with the increase in WCP replacement ratio.

3.2. Compressive strength (f_{cs})

The f_{cs} test results performed per the TS EN 196-1 standard are shown in Fig. 2(a). The f_{cs} test was performed on two pieces of samples obtained as a result of the f_{fs} test. For the mixture with each code, the average of the results of six samples was taken as the final f_{cs} result. The percentage of decrease in f_{cs} results of slag-based geopolymer mortars incorporating WCP compared to control geopolymer mortars without WCP is shown in Fig. 2(b).

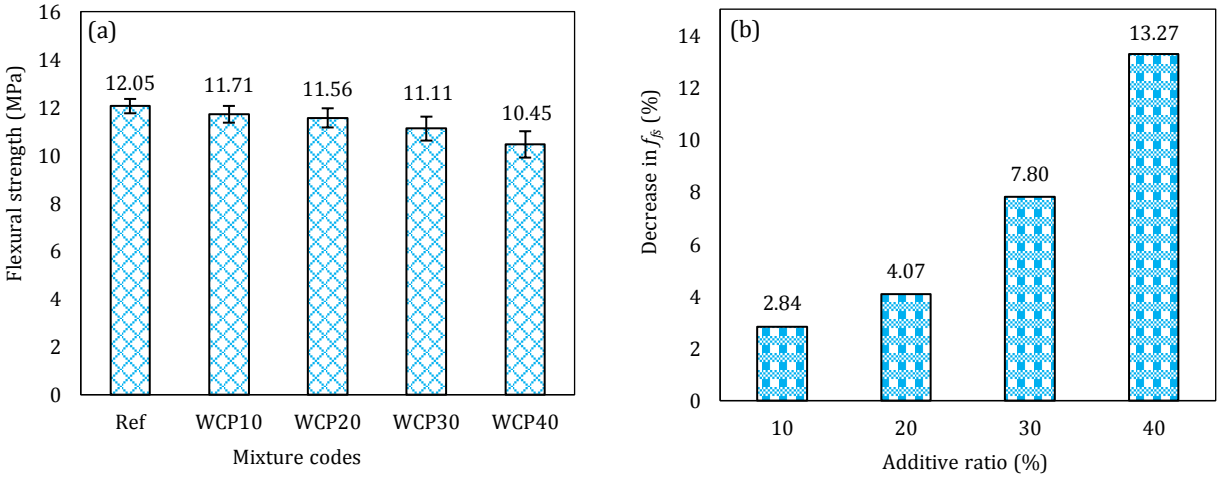

Fig. 1. (a) The f_{fs} test results;(b) The percentage of decrease in f_{fs} results.

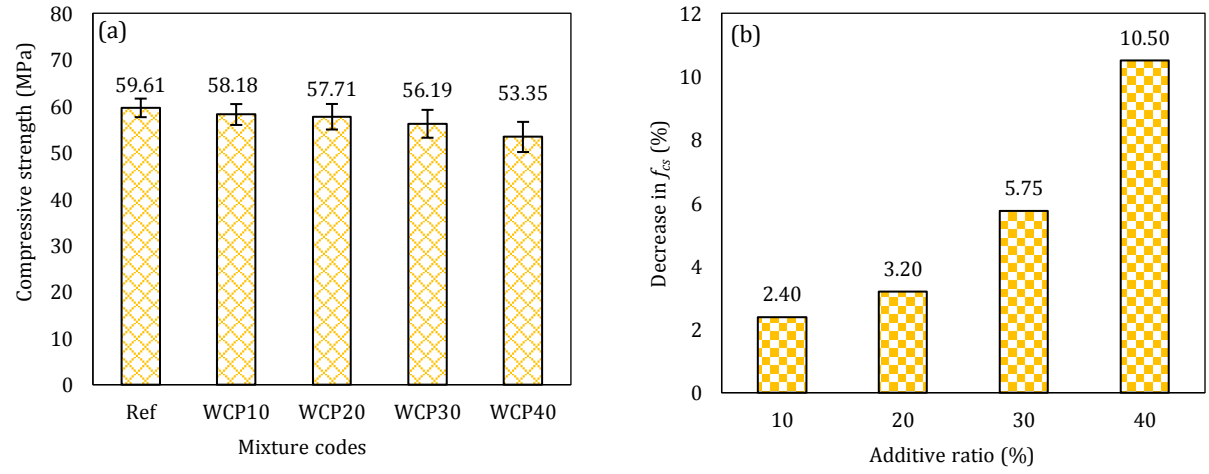

Fig. 2. (a) The f_{cs} test results; (b) The percentage of decrease in f_{cs} results.

When the f_{cs} results given in Fig. 2 are examined, it is seen that the f_{cs} results vary between 59.61 and 53.35 MPa. The f_{cs} results of the WCP10, WCP20, WCP30, and WCP40 decreased by 2.40, 3.20, 5.75, and 10.50%, respectively, compared to the Ref mortars. As in the f_{fs} results, the rate of decrease in the strengths increased with the increase of WCP replacement ratio in the f_{cs} results. However, considering the results obtained from the f_{cs} results, the f_{cs} results of all mixture groups remained above 50 MPa. This value is quite sufficient for many building applications. It has been noted that the slag adds more calcium oxide to the geopolymer matrix. Free calcium in the geopolymer matrix increases the reaction rate and the geopolymerization process due to the formation of C-A-S-H gel in the early stage (Puligilla and Mondal 2013; Tan et al. 2020). The reason for the decrease in f_{cs} results as a result of the increase in the replacement ratio of WCP in the geopolymer mortars can be explained in this way.

3.3. Ultrasonic pulse velocity (UPV)

The results of the UPV test performed per the ASTM C 597-16 standard are shown in Fig. 3(a). For the mixture with each code, the average of the results of three samples was taken as the final UPV results.

When the UPV results given in Fig. 3 are examined, it is seen that the UPV results vary between 4.55 and 4.29 km/h. The UPV results of the WCP10, WCP20, WCP30, and WCP40 decreased by 1.39, 2.75, 3.74, and 5.70%, respectively, compared to the Ref code mortars. As in the f_{fs} and f_{cs} results, the rate of decrease in the strengths increased with the increase of WCP replacement ratio in the UPV results. According to the Whitehurst (1951) classification, Ref mortars are in the "excellent" class, while WCP substituted mortars are in the "good" class. Song et al. (2019) reported that in geopolymer mortars, the slag can fill the pores and voids, thus increasing the strength of the matrix. For this reason, it was thought that the porosity of geopolymer mortars increased with the increase of WCP replacement ratio, and this situation caused decreases in UPV results. Fig. 4 shows the correlations between f_{fs} and f_{cs} results and UPV results. Linear regression was used to correlate the f_{fs} and f_{cs} results with the UPV results and the equations obtained are given on the graphs in Fig. 4. As seen in Figs. 4(a-b), R^2 values were obtained as 0.9641 and 0.9566, respectively. These values can mean good confidence in the correlation.

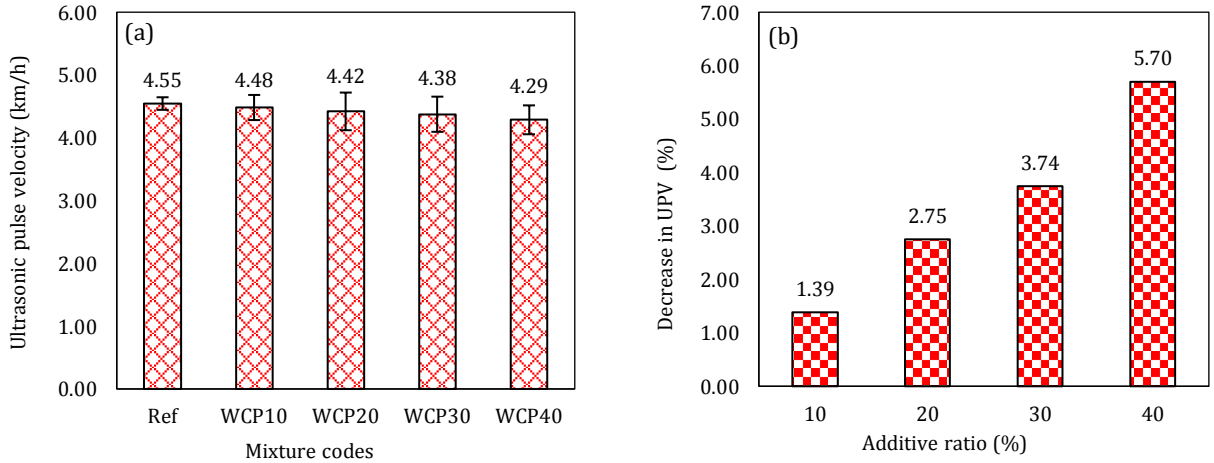

Fig. 3. (a) The UPV test results; (b) The percentage of decrease in UPV results.

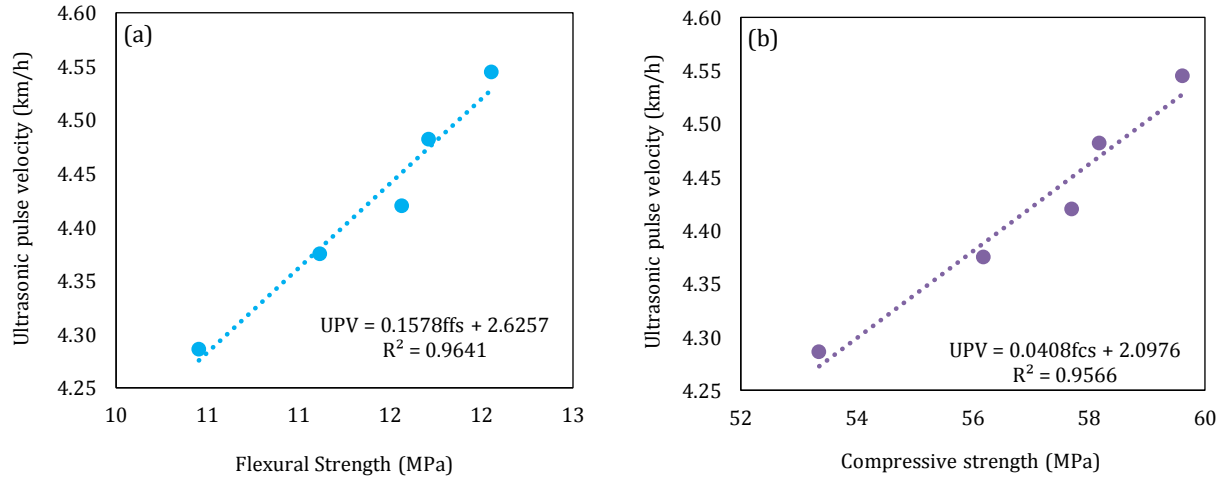

Fig. 4. Relationship between (a) f_{fs} and UPV; (b) f_{cs} and UPV.

4. Conclusions

In this study, the effect of waste concrete powder (WCP) on slag-based geopolymer composite mortars was investigated. Blast furnace slag (BFS) and WCP were used as binders in geopolymer mortars. WCP was substituted into the geopolymer mortar composites at rates of 10%, 20%, 30%, and 40% by weight of slag. Sodium hydroxide (NaOH) solution was used as the alkali activator in the mixtures and the solution activator concentration was chosen as 16 molars (M). After the prepared mortars were cured at 100°C for 24 hours, they were subjected to flexural strength (f_{fs}), compressive strength (f_{cs}), and ultrasonic pulse velocity (UPV) tests. The following results were obtained from this study:

- With the increase in WCP replacement ratio, decreases in f_{fs} ranging from 2.84 to 13.27% were observed. It has been determined that the decreases in f_{fs} results are seen more clearly when the replacement ratio rises above 20%. The highest strength loss was observed in geopolymer mortars with 40% WCP, and this rate was determined as 13.27%.
- f_{cs} results also decreased with the increase of WCP replacement ratio, similar to f_{fs} results. There were decreases in f_{cs} results between 2.40 and 10.50%. The lowest result in f_{cs} was obtained from geopolymer mortars with 40% WCP and was measured as 53.35 MPa. Although this result is 10.50% lower than reference mortars, it is a remarkably high value for many construction applications.
- When the UPV results were examined, it was seen that there were decreases between 1.39 and 5.70% with the increase in the WCP replacement ratio. However, according to the Whitehurst (1951) classification, mortars with WCP were found to be in the "good" class.
- Finally, it was determined that the relations between flexural strength & ultrasonic pulse velocity and compressive strength & ultrasonic pulse velocity parameters exhibited a remarkably high coefficient of determination (R^2).

When the results from the study are evaluated in general, it has been determined that WCP can be used in the remarkably high ratio (up to 40% replacement rate) in geopolymer mortars. Although it is seen that WCP replacement causes decreases in strength, it has been determined that the results are quite sufficient for many building applications. In addition, it has been observed that a high amount of WCP as a waste material can be disposed of using geopolymer mortars. In this way, environmental pollution will be reduced, and a sustainable environment will be contributed. In further studies, the effect of WCP can be examined by changing the molarity, curing temperature, and curing time parameters.

Acknowledgements

None declared.

Funding

The authors received no financial support for the research, authorship, and/or publication of this manuscript.

Conflict of Interest

The authors declared no potential conflicts of interest with respect to the research, authorship, and/or publication of this manuscript.

References

Ahmari S, Ren X, Toufigh V, Zhang L (2012). Production of geopolymeric binder from blended waste concrete powder and fly ash. *Construction and Building Materials*, 35, 718-729.

Alhawat M, Ashour A, Yildirim G, Aldemir A, Sahmaran M (2022). Properties of geopolymers sourced from construction and demolition waste: A review. *Journal of Building Engineering*, 50, 104104.

Bhutta MAR, Ariffin NF, Hussin MW, Lim NHAS (2013). Sulfate and sulfuric acid resistance of geopolymer mortars using waste blended ash. *Jurnal Teknologi*, 61(3), 1-5.

Çelikten S, Sarıdemir M, Akçaözoğlu K (2020). Effect of calcined perlite content on elevated temperature behaviour of alkali activated slag mortars. *Journal of Building Engineering*, 32, 101717.

Demir İ, Güzelkücük S, Sevim Ö (2018). Effects of sulfate on cement mortar with hybrid pozzolan substitution. *Engineering Science and Technology, an International Journal*, 21(3), 275-283.

Geraldo RH, Fernandes LF, Camarini G (2017). Water treatment sludge and rice husk ash to sustainable geopolymer production. *Journal of Cleaner Production*, 149, 146-155.

Li H, Deng Q, Zhang J, Xia B, Skitmore M (2019). Assessing the life cycle CO_2 emissions of reinforced concrete structures: four cases from China. *Journal of Cleaner Production*, 210(38), 1496–1506.

Mahmoodi O, Siad H, Lachemi M, Sahmaran M (2021a). Synthesis and optimization of binary systems of brick and concrete wastes geopolymers at ambient environment. *Construction and Building Materials*, 276, 122217.

Mahmoodi O, Siad H, Lachemi M, Dadsetan S, Sahmaran M (2021b). Development of optimized binary ceramic tile and concrete wastes geopolymer binders for in-situ applications. *Journal of Building Engineering*, 43, 102906.

Mahmoodi O, Siad H, Lachemi M, Dadsetan S, Şahmaran M (2022). Optimized application of ternary brick, ceramic and concrete wastes in sustainable high strength geopolymers. *Journal of Cleaner Production*, 338, 130650.

Mehta A, Siddique R (2017). Strength, permeability and micro-structural characteristics of low-calcium fly ash based geopolymers. *Construction and Building Materials*, 141, 325-334.

Meyer C (2009). The greening of the concrete industry. *Cement and Concrete Composites*, 31(8), 601-605.

Öztürk ZB, Atabey İİ (2022). Mechanical and microstructural characteristics of geopolymer mortars at high temperatures produced with ceramic sanitaryware waste. *Ceramics International*, 48(9), 12932-12944.

Provis JL (2014). Geopolymers and other alkali activated materials: why, how, and what? *Materials and Structures*, 47(1), 11–25.

Puligilla S, Mondal P (2013). Role of slag in microstructural development and hardening of fly ash-slag geopolymer. *Cement and Concrete Research*, 43, 70-80.

Qasrawi HY (2000). Concrete strength by combined nondestructive methods simply and reliably predicted. *Cement and Concrete Research*, 30, 739-746.

Rakhimova NR (2020). A review of calcined clays and ceramic wastes as sources for alkali-activated materials. *Geosystem Engineering*, 23(5), 287-298.

Rakhimova NR, Rakhimov RZ (2015). Alkali-activated cements and mortars based on blast furnace slag and red clay brick waste. *Materials & Design*, 85, 324–331.

Sahmaran M, Yildirim G, Erdem TK (2013). Self-healing capability of cementitious composites incorporating different supplementary cementitious materials. *Cement and Concrete Composites*, 35 (1), 89-101.

Sevim Ö, Demir İ (2019). Physical and permeability properties of cementitious mortars having fly ash with optimized particle size distribution. *Cement and Concrete Composites*, 96, 266-273.

Sevim O, Sengul CG (2021). Comparison of the influence of silica-rich supplementary cementitious materials on cement mortar composites: Mechanical and microstructural assessment. *Silicon*, 13(5), 1675-1690.

Shoaei P, Musaeei HR, Mirlohi F, Ameri F, Bahrami N (2019). Waste ceramic powder-based geopolymer mortars: Effect of curing temperature and alkaline solution-to-binder ratio. *Construction and Building Materials*, 227, 116686.

Song W, Yi J, Wu H, He X, Song Q, Yin J (2019). Effect of carbon fiber on mechanical properties and dimensional stability of concrete incorporated with granulated-blast furnace slag. *Journal of Cleaner Production*, 238, 117819.

Tahwia AM, Abd Ellatief M, Heneigel AM, Abd Elrahman M (2022). Characteristics of eco-friendly ultra-high-performance geopolymer concrete incorporating waste materials. *Ceramics International*, 48, 19662–19674.

Tan J, Cai J, Li X, Pan J, Li J (2020). Development of eco-friendly geopolymers with ground mixed recycled aggregates and slag. *Journal of Cleaner Production*, 256, 120369.

Thokchom S, Ghosh P, Ghosh S (2009). Acid resistance of fly ash based geopolymer mortars. *International Journal of Recent Trends in Engineering*, 1(6), 36.

Toklu K (2021). Investigation of mechanical and durability behaviour of high strength cementitious composites containing natural zeolite and blast-furnace slag. *Silicon*, 13(8), 2821-2833.

Toklu K, Şimşek O (2018). Investigation of mechanical properties of repair mortars containing high-volume fly ash and nano materials. *Journal of the Australian Ceramic Society*, 54(2), 261-270.

Ulugöl H, Kul A, Yıldırım G, Şahmaran M, Aldemir A, Figueira D, Ashour A (2021). Mechanical and microstructural characterization of geopolymers from assorted construction and demolition waste-based masonry and glass. *Journal of Cleaner Production*, 280, 124358.

Wang J, Li Z, Tam VW (2014). Critical factors in effective construction waste minimization at the design stage: a Shenzhen case study, China. *Resources, Conservation and Recycling*, 82, 1-7.

Whitehurst E (1951). Soniscope tests concrete structures. *Journal Proceedings*, 47(2), 433-444.